AMRL-TR-68-136

DEVELOPMENT OF SUPPORT AND RESTRAINT TECHNOLOGY

W. A. ROBBINS

G. L. POTTER

C. F. LOMBARD

Northrop Corporate Laboratories

APRIL 1969

JOINT NASA/USAF STUDY

AEROSPACE MEDICAL RESEARCH LABORATORY
AEROSPACE MEDICAL DIVISION
AIR FORCE SYSTEMS COMMAND
WRIGHT-PATTERSON AIR FORCE BASE, OHIO

NOTICES

When US Government drawings, specifications, or other data are used for any purpose other than a definitely related Government procurement operation, the Government thereby incurs no responsibility nor any obligation whatsoever, and the fact that the Government may have formulated, furnished, or in any way supplied the said drawings, specifications, or other data, is not to be regarded by implication or otherwise, as in any manner licensing the holder or any other person or corporation, or conveying any rights or permission to manufacture, use, or sell any patented invention that may in any way be related thereto.

Federal Government agencies and their contractors registered with Defense Documentation Center (DDC) should direct requests for copies of this report to:

DDC
Cameron Station
Alexandria, Virginia 22314

Non-DDC users may purchase copies of this report from:

Chief, Storage and Dissemination Section
Clearinghouse for Federal Scientific & Technical Information (CFSTI)
Sills Building
5285 Port Royal Road
Springfield, Virginia 22151

Organizations and individuals receiving reports via the Aerospace Medical Research Laboratories' automatic mailing lists should submit the addressograph plate stamp on the report envelope or refer to the code number when corresponding about change of address or cancellation.

Do not return this copy. Retain or destroy.

The experiments reported herein were conducted according to the "Guide for Laboratory Animal Facilities and Care," 1965 prepared by the Committee on the Guide for Laboratory Animal Resources, National Academy of Sciences—National Research Council; the regulations and standards prepared by the Department of Agriculture; and Public Law 89-544, "Laboratory Animal Welfare Act," August 24, 1967.

900 - July 1969 - CO455 - 84-1883

AMRL-TR-68-136

DEVELOPMENT OF SUPPORT AND RESTRAINT TECHNOLOGY

W. A. ROBBINS

G. L. POTTER

C. E. LOMBARD

FOREWORD

The work reported herein was performed by Northrop Corporate Laboratories, Hawthorne, California 90250, under joint Air Force and National Aeronautics and Space Administration sponsorship in accordance with USAF Contract F33615-67-C-1651. This work was performed in support of project 7231, "Biomechanics of Aerospace Operations," task 723101, "Effects of Vibration and Impact." Major George C. Mohr and Mr. Leon Kazarian of the Aerospace Medical Research Laboratory at Wright-Patterson Air Force Base, Ohio, were the successive contract monitors. Technical advice was also contributed by Mr. H.F. Scherer, NASA Manned Spacecraft Center, and Dr. John Billingham, NASA Ames Research Center. Dr. Charles F. Lombard served as principal investigator at Northrop.

The authors gratefully acknowledge the technical assistance of Mssrs. Rolf Neubert, George Branch, and Joseph Yonk in the conduct of animal experiments and operation of the decelerator facility; John Felder in overall engineering design and analysis of test facilities; Edward Nez, Annetto D'Aquila, and Ester Cook in design and fabrication of support-restraint systems; and Ralph Hubbard and James Schuessler for instrumentation support. Acknowledgement is also extended to Dr. S. H. Advani, currently of the University of West Virginia, for his contributions in theoretical analysis.

This technical report has been reviewed and is approved.

C. H. KRATOCHVIL, Colonel, USAF, MC
Commander
Aerospace Medical Research Laboratory

ABSTRACT

Guinea pigs were exposed to backward and forward facing ($\pm G_x$) and tail first ($+G_z$) impact accelerations in two types of support and restraint systems at entrance velocities of 40, 60, and 80 ft/sec. After exploratory experiments to determine the approximate 50% lethal G level (LD50), estimates of G levels for 40 and 60% mortality were made and 20 guinea pigs were exposed at each level. This was accomplished for each orientation at each velocity in each of the two systems. Using probit analysis, the refined LD50 G level was calculated and the results tabulated for comparison of the two systems for survival potential. Regarding protection, the system employing the isovolumetric principle was markedly superior in $+G_x$ impacts, slightly superior in $-G_x$ impacts, and approximately equal in the $+G_z$ orientation. Protection of the cardiovascular system by the isovolumetric system was markedly superior in $+G_x$ and $+G_z$ impacts but only slightly better in $-G_x$ impacts. Comparison of the two thoracic-abdominal systems was made possible by the concomitant use of a previously developed support and restraint system for the head. The LD50 values using average G ranged from 209 to 325 for $+G_x$, 287 to 350 for $-G_x$, and 103 to 135 for the $+G_z$.

TABLE OF CONTENTS

LIST OF FIGURES

LIST OF TABLES

SECTION I

INTRODUCTION

The development of support and restraint systems (henceforth referred to as SARS for convenience) for crew members of aerospace vehicles is an engineering task augmented by data obtained through biological investigation. These biological data provide the basis for design criteria which, in turn, establish the performance of an operational SARS. Comfort, efficiency, and survival, in that order, have been the key factors in evolution of the current SARS technology with engineers having made educated guesses where the biological data were lacking. This has led to the bioengineering type of research in which both the physical and biological sciences are used to study basic problems with the goal of providing adequate information for engineering design. With more adequate information it is hoped that design engineering activities could then develop SARS' that would permit higher vehicle performance specifications.

The basis for design for tolerance and survival during emergency and hard or crash landings has been a given G level (where G = acceleration/32.2) and a given direction of application. Unfortunately, the degree of rapid acceleration protection provided by current aerospace vehicle SARS involved in emergencies and hard or crash landings indicates that improvements are necessary.

The tolerance and survival limits of man to impact accelerations in the various orientations are known approximately, but only under certain conditions of support and restraint. The design principles upon which these SARS are based may not be entirely valid or complete enough to provide maximum protection in the system. Current systems using essentially flat torso supports and strap restraints for the pelvic and pectoral girdles and support, but no restraint for the head, depend greatly upon the strength of certain tissues to resist the distortion incurred by impact acceleration. In the $+G_x$ orientation the torso support permits the torso to distort or flatten out, especially in the abdominal area, with possible tension failure in various tissues in the viscera. In the $-G_x$ orientation without restraint, the inertia of the head and the abdominal contents places high tension loads on ligaments, fascia, and other tissues with potential injury directly or upon elastic rebound. In the $\pm G_y$ orientations the lack of sufficient restraint permits similar distortions, perhaps even more pronounced. In the $\pm G_z$ orientation the inherent weakness of the body has been more fully recognized with the result that the current SARS provide a relatively high degree of protection.

The accumulated evidence substantiates that man can withstand extremely high impact forces provided he is restrained and supported adequately. Stapp (1955, 1964) has shown that human volunteer subjects have peak G tolerance levels in excess of $-45G_x$, and $+35G_x$ with the

specific support and restraint system used. Snyder (1963) has analyzed data on 137 individuals who survived extremely abrupt impacts in free fall. These data show that man can survive impact forces considerably greater than those presently used as survival limits for design purposes. Using guinea pigs and monkeys, Lombard (1964a, 1966) isolated several significant factors that influence survival potential. By keeping the torso in a contoured support with an essentially full coverage restraint, a semi-isovolumetric condition for the torso was maintained during impact. Restraint of both the head and the torso in a manner to prevent sharp bending of the cervical spine and, use of a contoured and properly padded head support to prevent cerebral hemorrhage and skull fracture resulted in a substantial increase in survival to $+G_x$ impacts. The latter work indicated that survival from impact accelerations can be increased by proper orientation and containment of the body. The principles used in the design of support and restraint equipment responsible for this improved survival were evolved by finding the site and mechanism of injury through the correlation of pathology and forcing function parameters. A serious shortcoming of the work already performed, however, is the lack of statistical significance of the findings. This is largely due to the numerous permutations of impact variables (G, entrance velocity, orientation, and support-restraint, among others) and the corresponding requisite for large numbers of experiments. The present study was initiated to establish statistically valid data in a comparison of "isovolumetric" versus current state-of-the-art support-restraint concepts. Over 1200 small animals were exposed to impact in either the $+G_z$ (tail first), $-G_x$ (forward facing), or $+G_x$ (backward facing) orientations at entrance velocities of 40, 60, and 80 ft/sec using the two modes of support-restraint. The specific program objectives included determination of LD50 survival levels for guinea pigs, using the two representative support and restraint systems, and correlation of pathological change with impact acceleration parameters.

SECTION II

APPARATUS

The impact experiments were conducted on the Northrop Horizontal Decelerator (see figure 1). The decelerator facility includes a sled with means for containing various support and restraint systems (SARS), a track upon which the sled travels, a shock cord propulsion system that accelerates the sled, and an anvil-inertia block that retains the crushable material used to rapidly decelerate the sled and its contents. The aluminum-magnesium composition sled features an adjustable yaw ring that allows positioning of the installed SARS 360° about the vertical axis. The particular SARS is attached to the yaw ring via two trunions that permit adjustment of subject pitch through 360°. Desired impact orientations can be achieved by various combinations of yaw and pitch adjustments. The sled track consists of two steel rails 30 feet in length and spaced 30 inches apart. A steel anvil is mounted on a 20-ton steel reinforced concrete inertial mass located at the end of the sled track. The anvil contains means for mounting and retaining metal honeycomb column(s) that provide controlled impact deceleration when crushed by the oncoming sled. Sled propulsion is accomplished by a length of shock cord (bungee) in tension. The amount of tension (controlled by a power winch) and the location of the sled release point determine the entrance velocity. The term "entrance velocity" as used in this work refers to the final sled velocity at the initial point of sled-honeycomb contact. Entrance velocity measurement was accomplished by detecting the average sled velocity over the last 3 inches of travel (before honeycomb impact). A velocity term often used in connection with impact is velocity change (ΔV) or entrance velocity plus rebound velocity. In the experiments described herein at 40, 60, and 80 ft/sec entrance velocities, the corresponding velocity change values were approximately 50, 70, and 90 ft/sec, respectively.

This decelerator facility is capable of producing deceleration pulses up to 1200 peak G. Attainable entrance velocities range from 20 to 100 ft/sec with corresponding velocity changes (ΔV) from 30 to 110 ft/sec. The range of attainable impact durations is a function of G and velocity and may be determined for specific values using

$$t = \frac{\Delta V}{G \cdot 32.2} \qquad (1)$$

where
ΔV = velocity
$G = a/g$

The characteristic pulse shape may be varied in rise time or onset by appropriately configuring the impact face of the honeycomb column although this was not necessary for the work described herein. Near rectangular

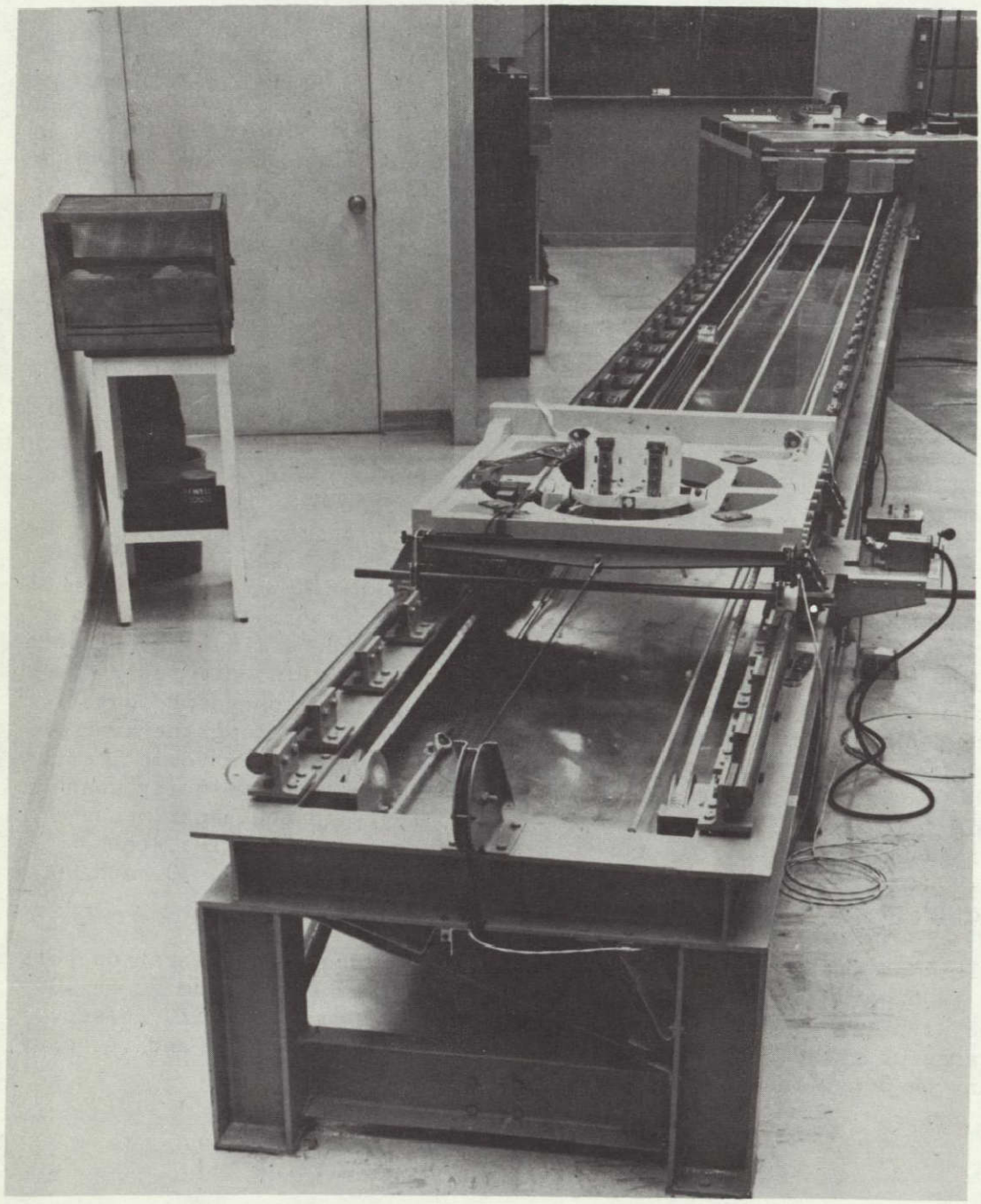

FIGURE 1 Northrop Horizontal Decelerator Facility Viewed from Breech End with Sled in Firing Position. Anvil with Honeycomb Mounted and Inertia Block are Visible at End of Track in Background.

pulses can be achieved with flat face honeycomb columns up to $\approx$ 500 G. In and above this regime, the pulse assumes a more trapezoidal shape because of the short peak deceleration times. Deceleration pulses typical of flat or near flat face aluminum honeycomb column impacts over the G range explored in this work are shown in figure 2. The type of honeycomb used in this work was aluminum 5052 alloy, 0.003 inch foil thickness, and 0.1875 inch cell diameter, conforming to military specification MIL-C-7438C. The approximate density and compressive strength of this material was 8 lb/cu ft and 1200 psi, respectively. Sled acceleration down the track is relatively constant and ranges from two to four G, depending on the preset of the bungee cord to provide the desired impact entrance velocity. A typical down-the-track acceleration profile is also given in figure 2D. The bungee, or rubber strand shock cord, used to propel the sled , included first 0.75-inch and then 1.0-inch-diameter types (MIL-C-5651); the smaller cord was used for the 40 ft/sec experiments. In general, a single, 120-foot length of either 0.75- or 1.0-inch cord was installed in the decelerator apparatus through several pulleys and a winch tensioning system. The winch was then used to adjust bungee tension from slack to 50% elongation (with the sled resting against the anvil). Retraction of the sled to the furthermost position down the track provided an additional 50% bungee elongation. The maximum bungee tension was, therefore, 100% elongation including both preload tension and sled retraction tension. Typical load values (measured with a tension strain gage) for the 1.0-inch cord tensioned via sled retraction (with no preload tension) were 580 pounds at 12% elongation, 700 pounds at 25%, and 980 pounds at 50%. During experiment operations the sled release point was located at a point along the track distant enough from the anvil to provide the approximate desired entrance velocity. Adjustment of bungee preload and test runs enabled the final setting for the desired velocity.

Shortly after the decelerator was installed in this laboratory, tests were conducted to determine low frequency resonance spectra of the intact sled structure. Using a large scale electrodynamic shaker equipment, the sled (with one of the SARS included) was subjected to sinusoidal vibration from 0 to 700 Hz in the direction of sled impact. Three resonance modes were observed, namely; 355 Hz = 4 F, 600 Hz = 2 F, and 640 Hz = 10 F where xF is the amplification of the input force F. The approximately equivalent single-pulse periods are 3.0, 1.6, and 1.5 msec, respectively. Analysis of the actual impact pulse rise and decay times (τ) obtainable with the current apparatus indicates that the worst case with respect to sled resonance (most rectangular pulse) still provides a large enough τ to effectively avoid excitation of the higher frequency resonance modes.

The required impact acceleration levels were obtained by accelerating the sled (containing one set of the two SARS) up to a given velocity, whereupon contact and crushing of a specifically configured honeycomb column occurred. The relationships used to find the specific honeycomb column dimensions for a required impact level are

$$G = \frac{F_{cr} A}{W} \qquad (2)$$

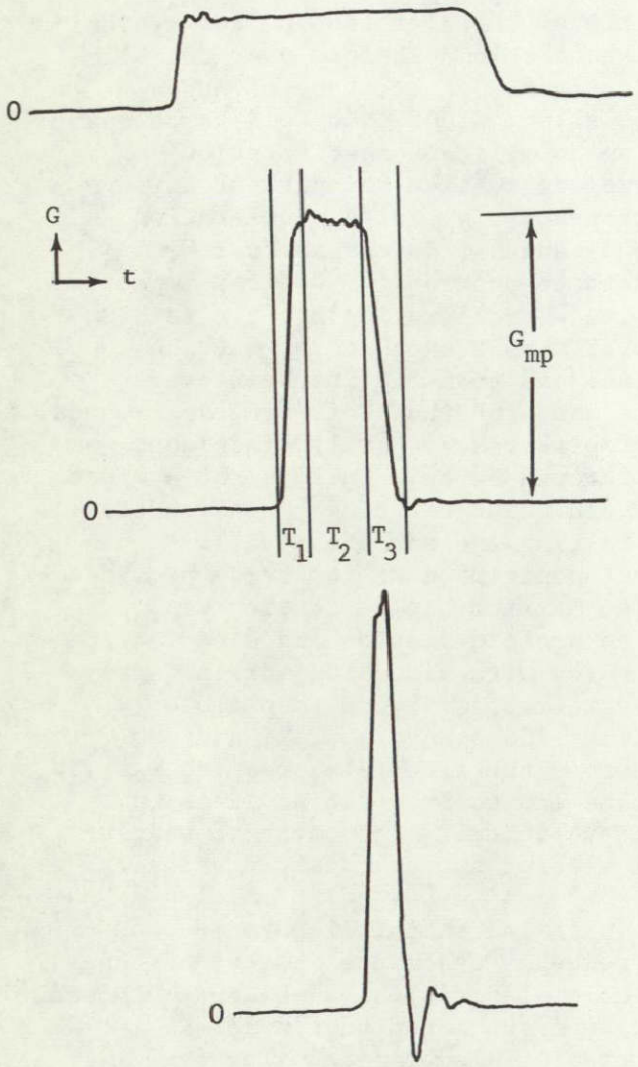

A

$G_{mean\ peak}$ = 95
G_{avg} = 86
t = 33 ms
onset = 62.000 G/sec

B

$G_{mean\ peak}$ = 300
G_{avg} = 237
t = 11.5 ms
onset = 175,000 G/sec

C

$G_{mean\ peak}$ = 600
G_{avg} = 357
t = 4.2 ms
onset = 420,000 G/sec

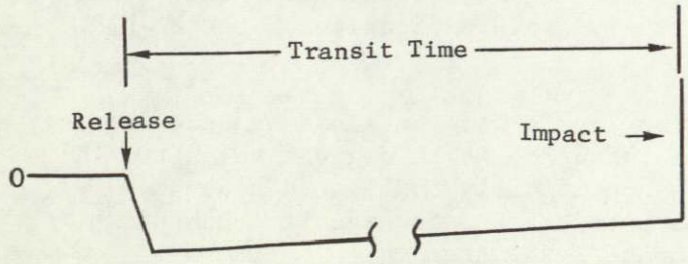

D

Peak Transit G (initial) = 4.0
Avg. Transit G = 3.6
Transit G at impact = 3.1
Entrance Velocity = 40 ft/sec
Total Transit t = 420 ms

FIGURE 2 Typical Impact Pulses and Sled Transit Data for Northrop Horizontal Decelerator.

where

F_{cr} = honeycomb compressive strength (along cell axis), psi

A = honeycomb column impact face area, $in.^2$

W = total weight of sled, lb

G = desired impact G level ($G = \frac{a}{32.2}$)

and

$$S = \frac{V^2}{2Gg} \tag{3}$$

where

S = amount of honeycomb column crush (along cell axis), in.

V = entrance velocity, ft/sec

$g = 32.2\ ft/sec^2$

For a given required G level then, the honeycomb face area was calculated using the known steady state compressive strength of the particular honeycomb in use. The final length of the column after crushing was then determined. Addition of a safety factor of 3 inches to this value gave the minimum column length permissible for the particular test. At the higher G levels, a slight contour was cut on the column impact face to reduce the high frequency shock produced at the onset of crushing. At these high G levels the extreme initial shock with a flat face column could damage or destroy the impact accelerometer.

Instrumentation for detecting and recording the deceleration pulse consisted of an Endevco Model 2261C $\pm$ 2500 G piezoresistive acceleration transducer and a CEC recording oscillograph (Model 5-124) using a CEC 7-342 galvanometer with a frequency response of 0 to 135 Hz. The paper speed used in this work was 64 inches per second. The output of the accelerometer was calibrated and fed through a balance box to the oscillograph. Entrance velocity was determined over the last 3 inches traveled by the sled to break two in-line electrical circuits. The time pulse was recorded on the oscillograph as well as displayed on a Hewlett-Packard electronic counter Model No. 5223L. The acceleration data obtained reflect sled acceleration only, since the impact accelerometer was mounted on a cross member of the sled structure. A small number of experiments ($\pm G_x$ impacts) were carried out with an Endevco Model 2264M1 subminiature accelerometer taped to the animal's sternum. Although the restraint further stabilized this mounting, the rigidity of the attachment was still less than that required for obtaining highly accurate data. The data obtained from this arrangement were therefore used for subjective comparison only.

SECTION III

SUPPORT AND RESTRAINT SYSTEMS

The two Support and Restraint Systems (SARS) used in this work are designated SARS IIa and SARS IIIa. SARS IIa represents the compromised isovolumetric concept, while SARS IIIa approximates the current state-of-the-art in aerospacecraft-type support-restraint. The II and III nomenclature stems from previous related SARS developed and studied by this laboratory and reported on in the literature. SARS I (not used in this work) was the earliest isovolumetric type system developed by this laboratory and consisted of a fully enclosing rigid shell molded to the guinea pig's surface. This system is described in full by Lombard (January 1964). The original SARS II and III are also described by Lombard (January and September 1964); the IIa and IIIa systems used in this work differ in the type of restraint harnesses employed.

SARS IIa essentially consisted of a rigid, contoured support and a one-piece fabric apron-type thoracic-pelvic restraint (see figure 3). The support was fabricated from fiberglass molded to the guinea pig dorsal surface. The molded fiberglass shell was attached to a steel box and the box innerspace filled with high-density rigid polyurethane foam. The accompanying restraint harness was designed to cover the principal ventral thoracic-abdominal area of the guinea pig. The harness was constructed of 0.50-inch-wide Nylon web strap overlaid with Dacron cloth as shown in figure 4. Retention straps were provided in the shoulder, upper chest, lower abdominal, and crotch regions. Clamp-type retainers located on the rear surface of the support secured the straps. The guinea pig's head was restrained with an open-ended cone-shaped mask retained at ear level on both sides and at the top or crown (see figure 5) The head restraint was fabricated of Dacron cloth and Nylon web strap. During the initial experiments a 0.25-inch-thick pad of resilient foam was secured to the contoured support in the head region. Because of a high incidence of brain hemorrhage that occurred where this arrangement was used, the head pad was changed to 0.50-inch-thick rigid foam (contoured to the head as well as the support). This pad was used throughout the remainder of the experiments.

The SARS IIIa support was fabricated from sheet steel and consisted of flat plates for the back support and the seat portion at 90° to the back (see figure 6). The restraint harness used with this support differed from the SARS IIa restraint in two important respects (see figure 7). First, no overlaid material was used; the 0.50-inch-wide web strap geometry was otherwise identical. Second, the SARS IIIa restraint was a two-piece assembly; the abdominal-crotch webbing was physically separate from the thoracic webbing. The head restraint used on SARS IIIa was the same as that used with SARS IIa. As with the SARS IIa head support, the IIIa initially had only a 0.25-inch-thick pad of resilient

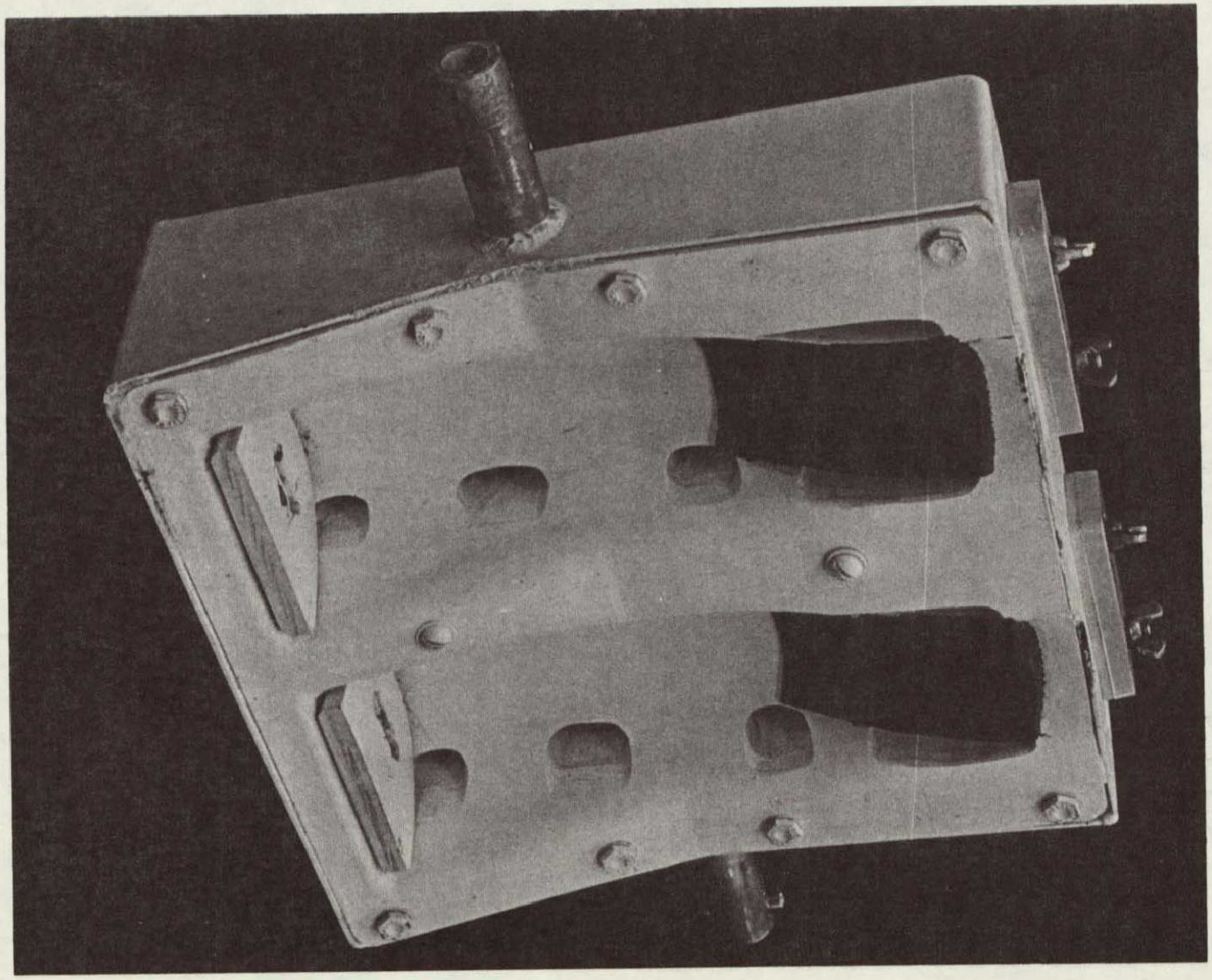

FIGURE 3 Three-Quarter View of Contoured SARS IIa Support with Nonresilient Foam Pads Located in Head and Neck Region.

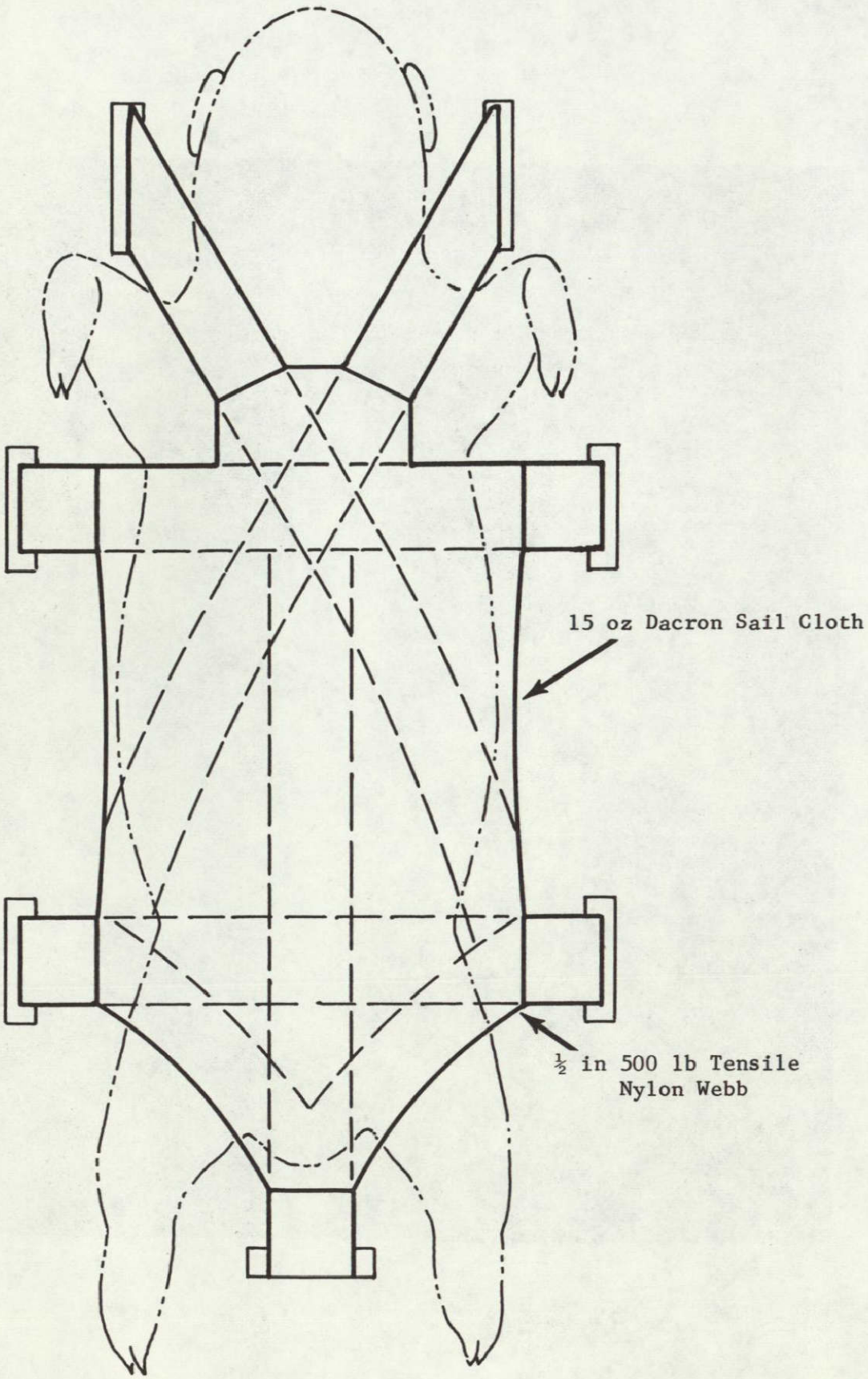

FIGURE 4 SARS IIa Restraint Harness Layout and Installation for the Guinea Pig.

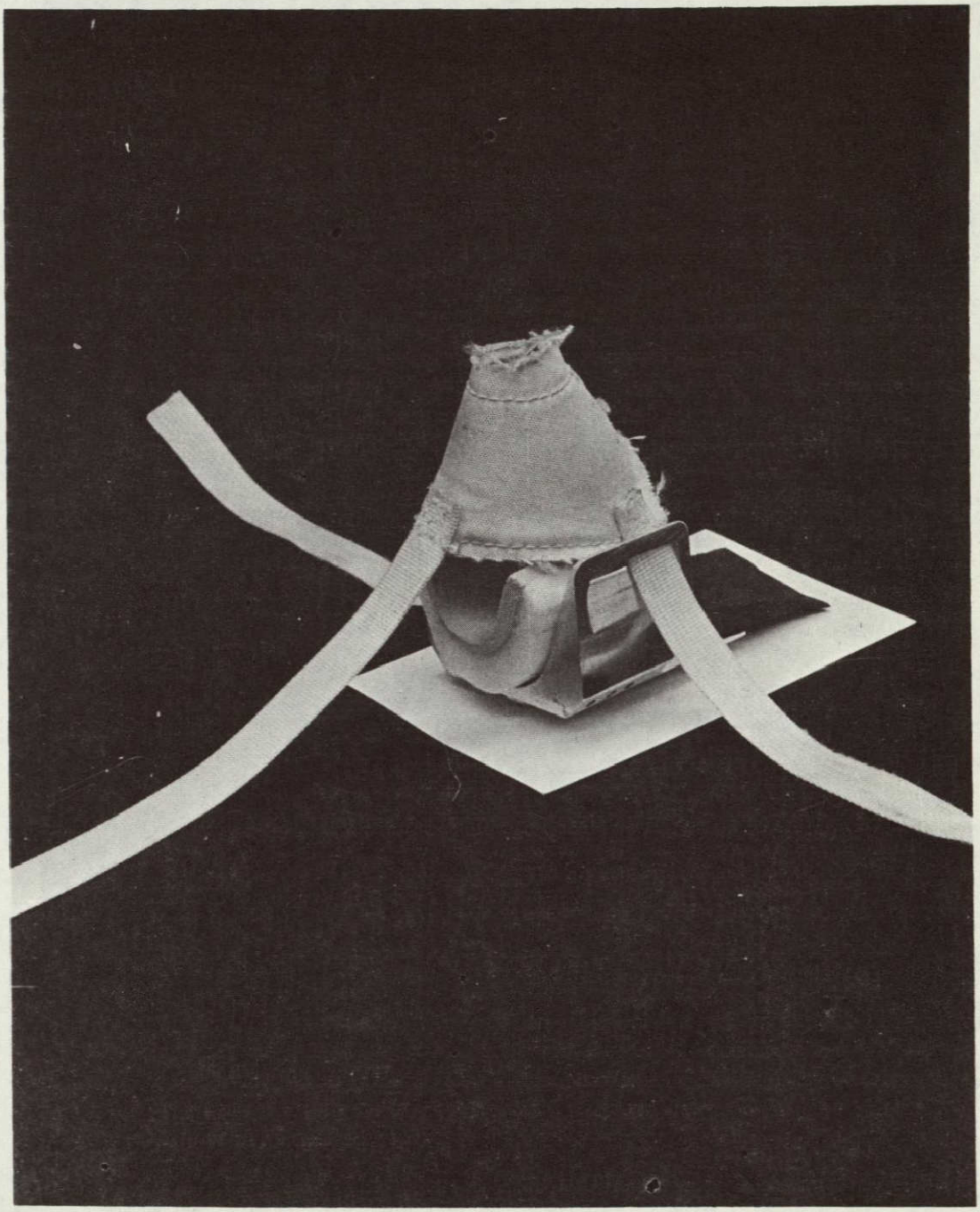

FIGURE 5 Three-Point Cloth Cone Head Restraint Used with both SARS IIa and IIIa (Shown in place in SARS IIIa Head Support Bracket).

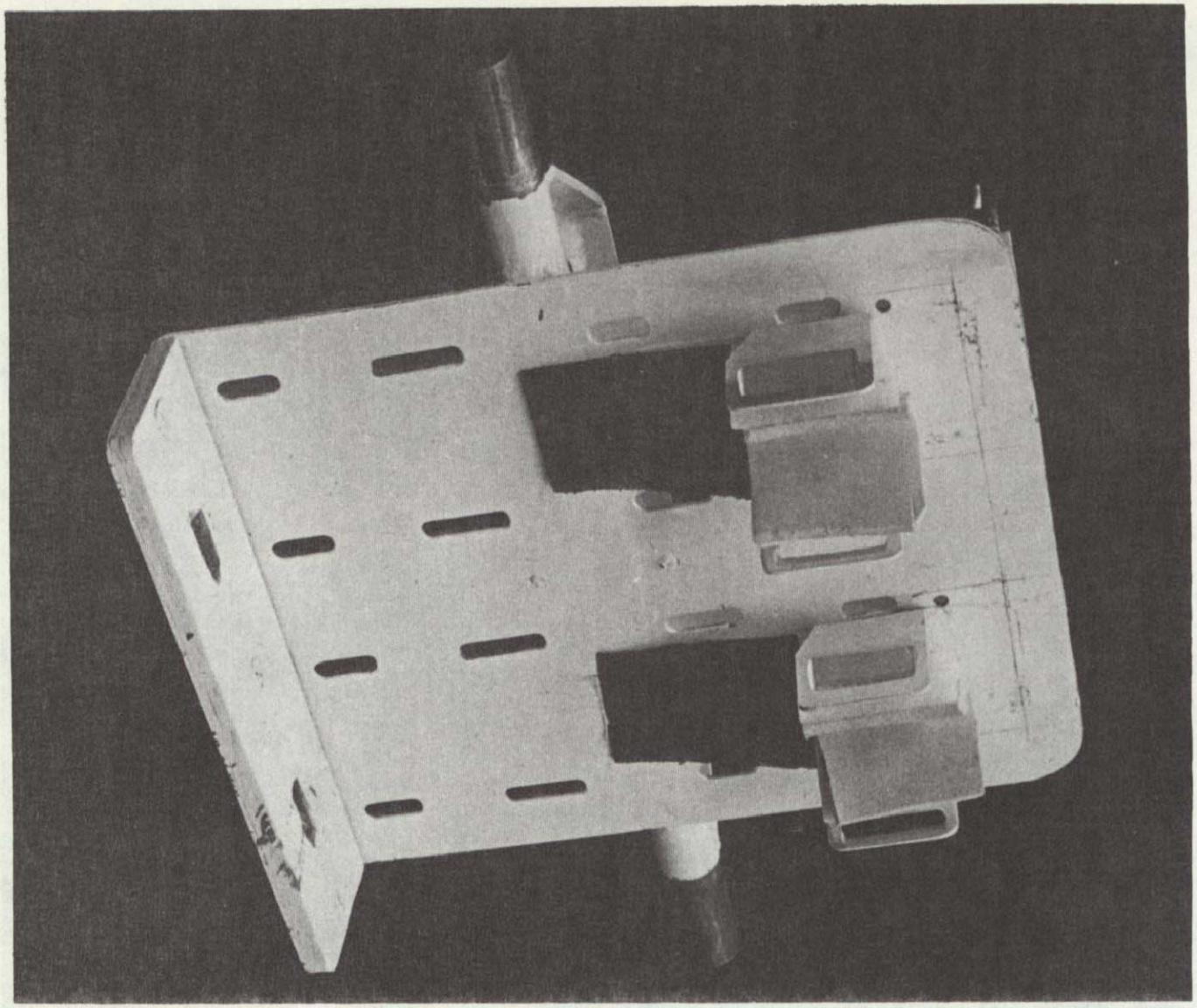

FIGURE 6 Three-Quarter View of SARS IIIa Support with Head Support Bracket in Place.

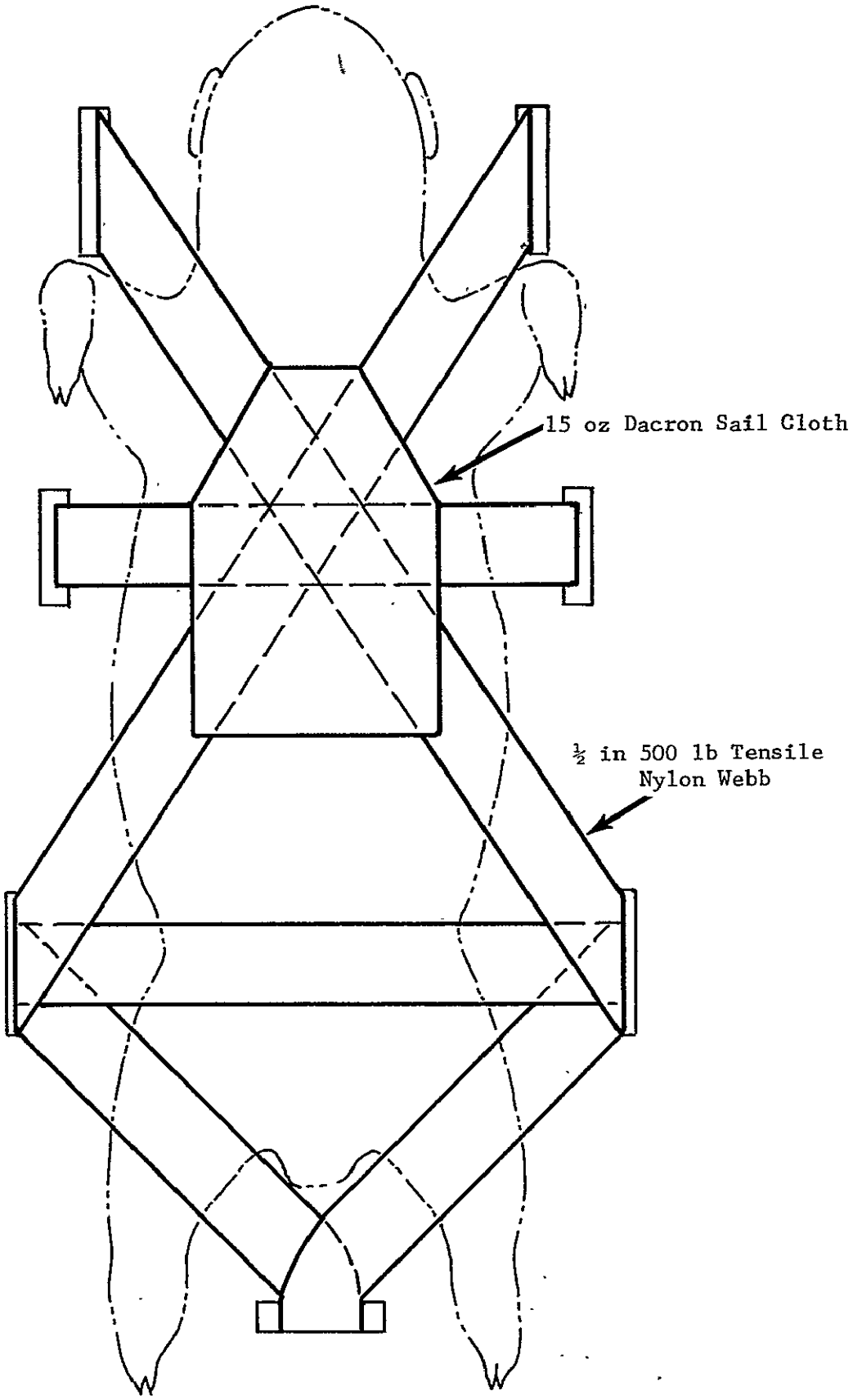

FIGURE 7 SARS IIIa Restraint Harness Layout and Installation for the Guinea Pig.

foam bonded to the flat plate in the head region. This was soon modified, for the reason given earlier. The final SARS IIIa head support was composed of a contoured aluminum bracket and a correspondingly contoured 0.50-inch-thick rigid foam insert.

Both types of SARS were fabricated and mounted on the sled in duplicate to accommodate two animals each in side-by-side fashion, allowing exposure of two subjects to impact in the same type of SARS per each sled firing.

SECTION IV

PROCEDURE

The specified impact exposure parameters combined with the two modes of support-restraint resulted in 18 sets of test conditions. In order to determine the lethal impact dose for 50% of the subject animal population (LD50) an exploratory group, of up to ten guinea pigs, was exposed to increasing dose levels until a 50% mortality level was approximated. Twenty animals were then exposed to a G level estimated to be 10% higher than the exploratory 50% mortality dose ($\approx$LD50) or an approximate LD60, and another 20 animals exposed to an approximate LD40 ($\approx$LD50 - 10%) G level. The actual LD values from these two groups of experiments were analyzed, using the probit regression line technique and the actual LD50 level determined for the particular SARS, orientation, and velocity combination. The LD50 data for both SARS IIIa and IIa were then plotted against G level and duration of impact (for each orientation) to provide G-t curves and concomitant energy transfer data.

The guinea pigs used in this investigation ranged in weight from 300 to 400 g. The animals were fasted for 24 hours before impact. The guinea pigs were placed in the SARS just before the decelerator was readied for firing. SARS strap tension and general fit was snug but not to the point of impeding respiration or circulation. Immediately post-exposure, rapid observation was made for SARS failure and obvious trauma. The animals were then quickly removed and placed in a prone position. All exposed animals were weighed immediately postimpact. Subjects that expired were autopsied within 30 minutes. Live animals were replaced in cages with food and water and observed for 24 hours. Animals that did not die within 24 hours were considered survivors. Those animals exhibiting paralysis for over one hour postexposure were considered nonsurvivors and euthanized.

The autopsy procedure for gross pathology included macroscopic examination of the abdominal and thoracic contents, ribs, vertebral column, and brain. A midline incision of the dermis was made from just above the genital opening to the neck region. The dermis was separated from the muscle layers via blunt dissection. The skin and muscle layers of abdomen and thorax were examined for gross pathology. The muscle layers were then incised along the midline exposing the abdominal viscera. The viscera were inspected and gross pathological changes noted. Thoracic viscera were exposed by incising the diaphragm, ribs, and intercostal muscles and reflecting the sternum. Thoracic viscera were inspected for gross pathology. Thoracic and abdominal viscera were then removed and the vertebral column was examined for signs of injury (fractures and dislocations). Heads were removed from the body, skinned, and fixed in a 10% formalin solution for at least 7 days. This storage period facilitated the identification of hemorrhage resulting from the impact.

At the end of the period the heads were rinsed with water, the cranium opened, and the brain examined for signs of injury. In this way blood vessel disruption caused by opening the cranium would not be confused with that caused by impact.

SECTION V

RESULTS

The acceleration force expression chosen for the LD50 analysis was the total applied impact force averaged over the total pulse duration. This expression, G_{avg}, provides a good measure of total force applied and, in combination with the duration, an accurate representation of energy, particularly when the impact pulse is other than an ideal rectangular envelope. A practical compromise requiring that the measuring accelerometer be located on the sled rather than on the test subject qualifies the data somewhat; however, this arrangement is not without precedent (Lombard, January 1964).

Summarized data for the 18 test groups relating mortality, velocity change, G, duration and onset are given in tables I, II, and III. The body of statistically significant data represents 720 impact exposures. Over 1200 animals were exposed in obtaining these data. Many of the additional animals were used in approximating the LD50 levels and in achieving the 5% accuracy for exposure iterations at the same G level. Derivation of the regression equation for each set of LD points at the same velocity change allowed calculation of the 50% lethal dose. Regression lines corresponding to these equations are given in figures 8 through 13 for each set of test conditions. The LD50 values obtained from the statistical data are given in table IV. Each LD50 value represents 40 exposures; 20 at one mortality G level and 20 at a second level. Applying the method described by Finney (1962) for determining fiducial or confidence limits shows a 95% confidence interval of approximately $\pm$ 17% for the LD50 mortality values. In other words, in 95% of n number of repeated trials at a given LD50 G level, mortality would range no lower than 33% and no higher than 67%. The G-t curves for LD50 G levels are plotted for each orientation in figures 14, 15, and 16. These curves effectively present the energy versus 50% mortality relationship over the range of impact durations studied. Gross pathology data for the 341 nonsurvivors (out of the 720 subject total) are tabulated in tables V, VI, and VII. The tables are divided into injury categories of frequent or significant occurrence. This delineation includes injuries of the following nature: pulmonary, cardiovascular, hepatic, gastrointestinal, paralysis, and miscellaneous. Table VIII gives the time of death after impact exposure for all nonsurvivors.

The impact acceleration data oscillograph recordings were reduced by hand to give mean peak or plateau G (G_{mp}), time of onset or rise time (T_1), time of plateau (T_2), time of offset or decay time (T_3), and total pulse time (see figure 8). Average G (G_{avg}) was calculated from

$$G_{avg} = G_{mp} \frac{T_1 + 2T_2 + T_3}{2(T_1 + T_2 + T_3)} \qquad (4)$$

TABLE I . SUMMARIZED IMPACT DATA FOR +G ORIENTATION, SARS IIIa and IIa

ΔV	V_e	LD%	G Average	G Plateau	t (ms)	Onset G x 1000/sec
SARS IIIa						
48	40	15	184	257	8.1	143
52	40	65	220	318	7.3	167
70	60	55	240	317	9.1	180
71	60	85	282	394	7.8	225
92	80	25	239	304	11.6	189
89	80	65	288	383	9.6	227
SARS IIa						
48	40	20	276	443	5.4	292
52	40	55	327	539	4.9	341
68	60	45	311	444	6.8	323
71	60	85	363	548	6.1	380
91	80	40	302	379	9.4	292
91	80	90	347	460	8.1	359

TABLE II. SUMMARIZED IMPACT DATA FOR $-G_x$ ORIENTATION, SARS IIIa AND IIa

SARS IIIa						
ΔV	V_e	LD%	G Average	G Plateau	t (ms)	Onset G x 1000/sec
49	40	30	260	450	5.9	260
60	40	70	317	513	5.9	292
70	60	50	315	483	6.9	296
73	60	90	368	587	6.2	360
95	80	55	310	417	9.5	258
94	80	90	351	508	8.2	282
SARS IIa						
47	40	30	286	484	5.1	299
49	40	60	347	593	4.4	429
70	60	10	293	409	7.2	291
72	60	40	338	484	6.6	360
94	80	50	311	404	9.4	343
92	80	75	353	482	8.1	378

TABLE III SUMMARIZED IMPACT DATA FOR $+G_z$ ORIENTATION, SARS IIIa and IIa

ΔV	V_e	LD%	G Average	G Plateau	t (ms)	Onset G x 1000/sec
SARS IIIa						
47	40	35	83	96	17.6	118
47	40	45	96	113	15.2	128
68	60	25	100	112	21.2	83
70	60	50	116	131	18.7	90
89	80	20	99	109	28.0	83
88	80	35	117	131	23.4	95
SARS IIa						
50	40	25	87	100	17.9	54
47	40	40	104	124	14.0	67
74	60	30	98	110	23.4	58
74	60	55	114	130	20.1	80
92	80	10	88	95	32.4	68
89	80	40	106	116	26.0	88

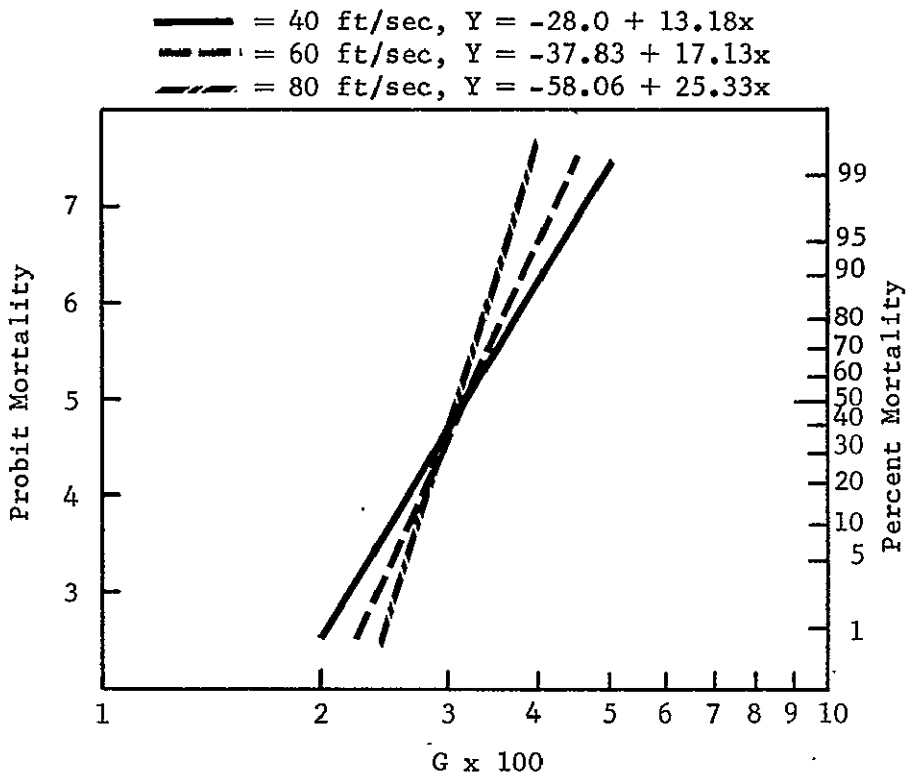

FIGURE 8 Mortality versus G at Three Entrance Velocities, $+G_x$, SARS IIa.

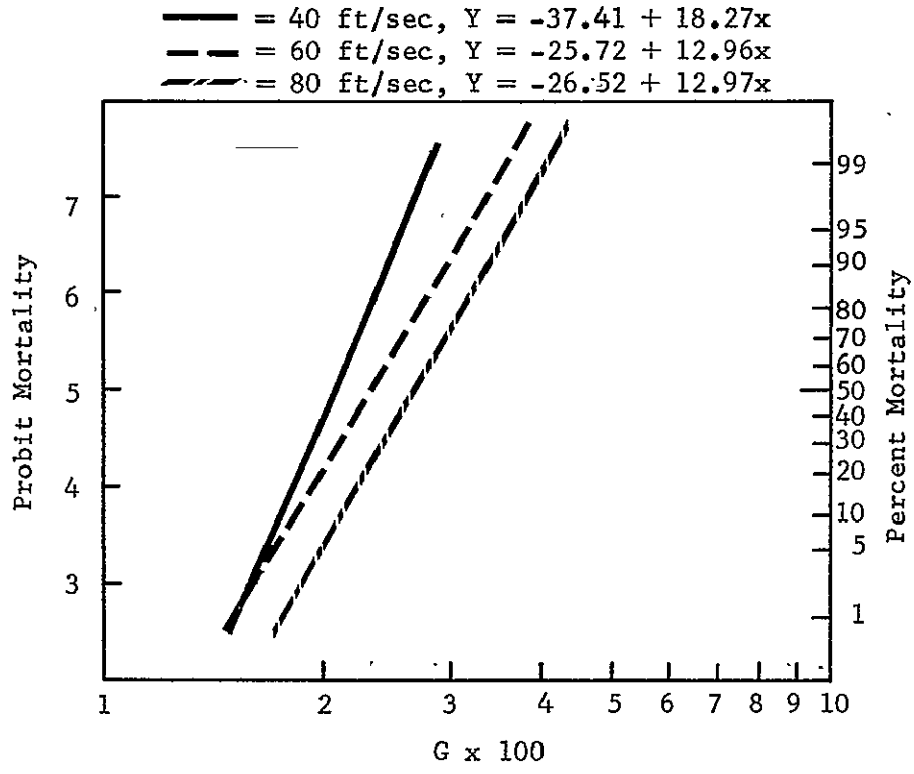

FIGURE 9 Mortality versus G at Three Entrance Velocities, $+G_x$, SARS IIIa.

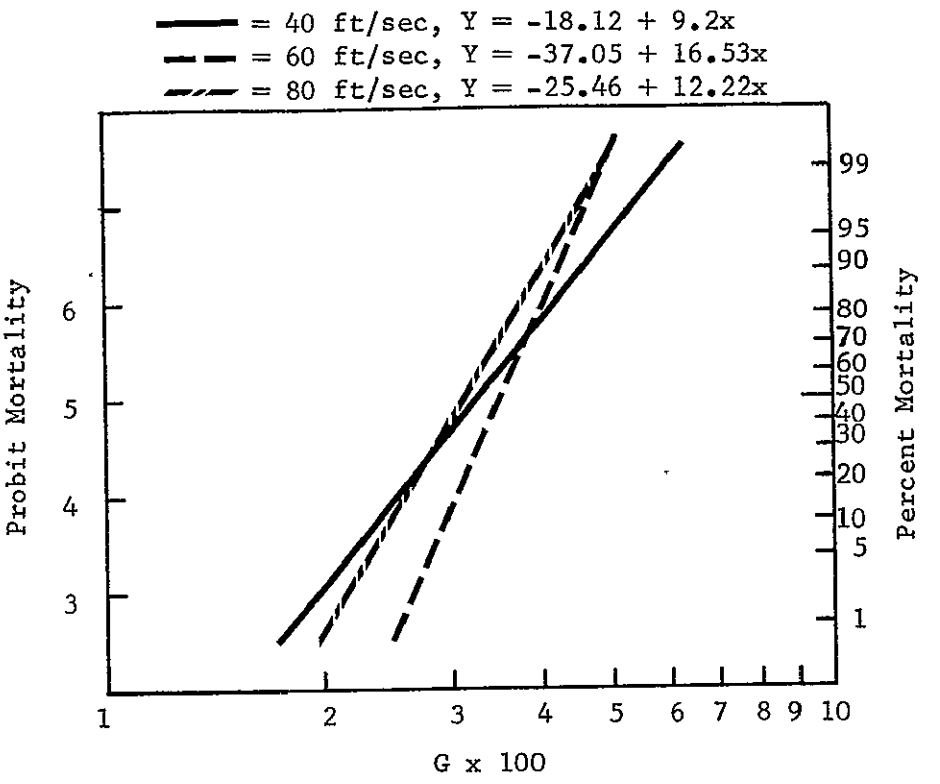

FIGURE 10 Mortality versus G at Three Entrance Velocities, $-G_x$, SARS IIa.

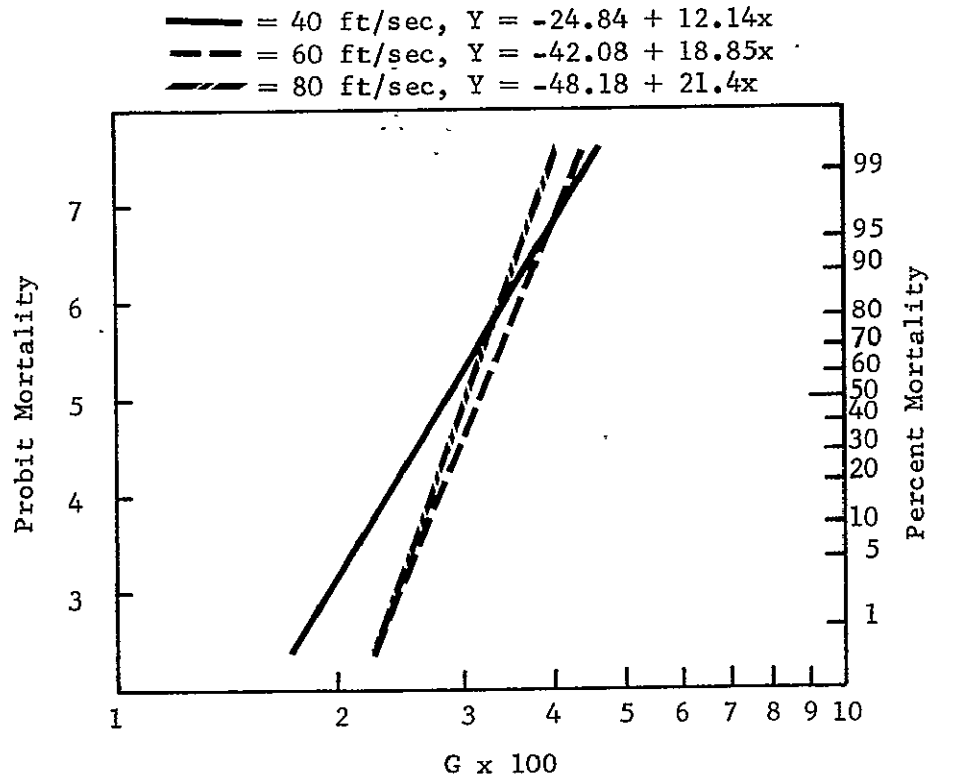

FIGURE 11 Mortality versus G at Three Entrance Velocities, $-G_x$, SARS IIIa.

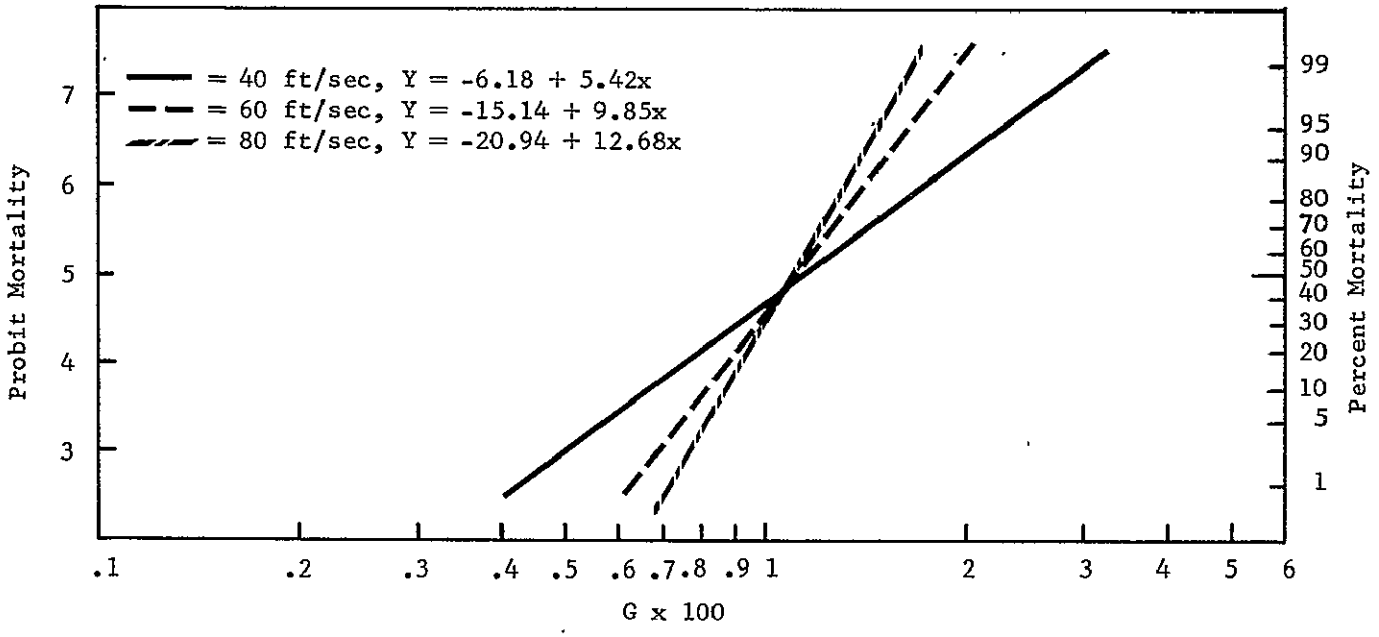

FIGURE 12 Mortality versus G at Three Entrance Velocities, $+G_z$, SARS IIa.

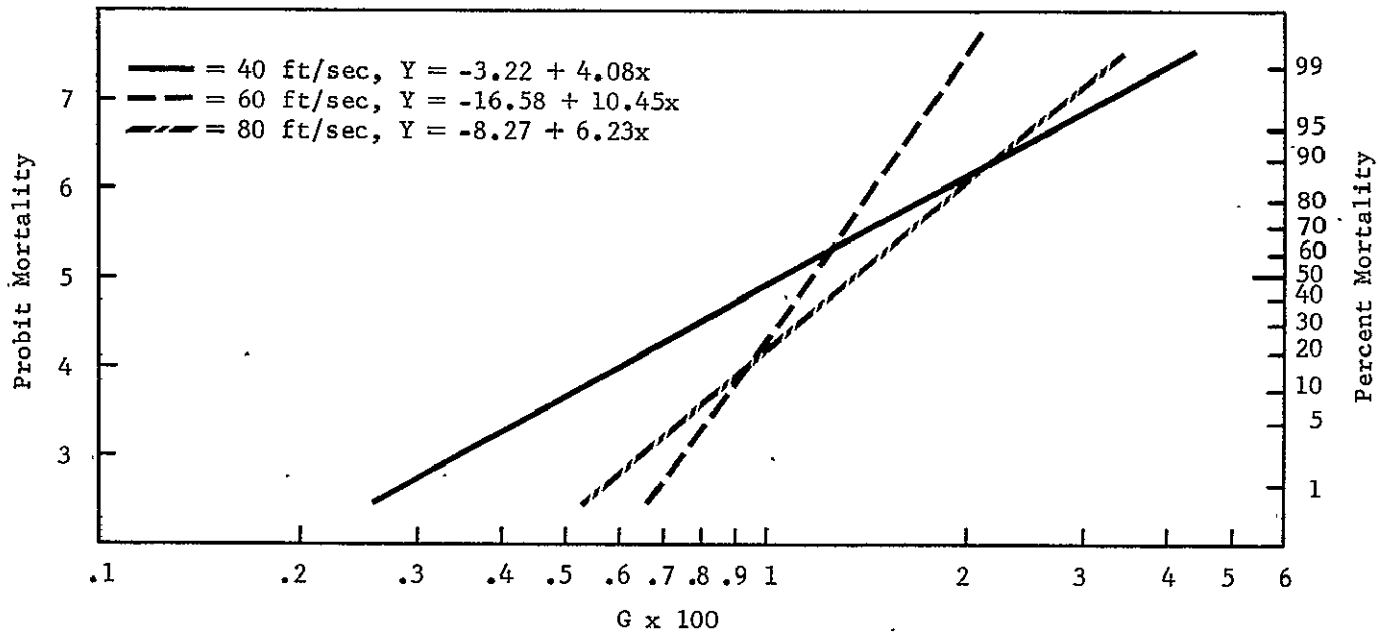

FIGURE 13 Mortality versus G at Three Entrance Velocities, $+G_z$, SARS IIIa.

TABLE IV AVERAGE G LD50 VALUES USING PROBIT INTERCEPT

V_e	SARS IIIa			SARS IIa		
	$+G_x$	$-G_x$	$+G_z$	$+G_x$	$-G_x$	$+G_z$
40	209	287	103	326	325	116
60	235	315	116	316	350	111
80	269	306	135	309	311	111

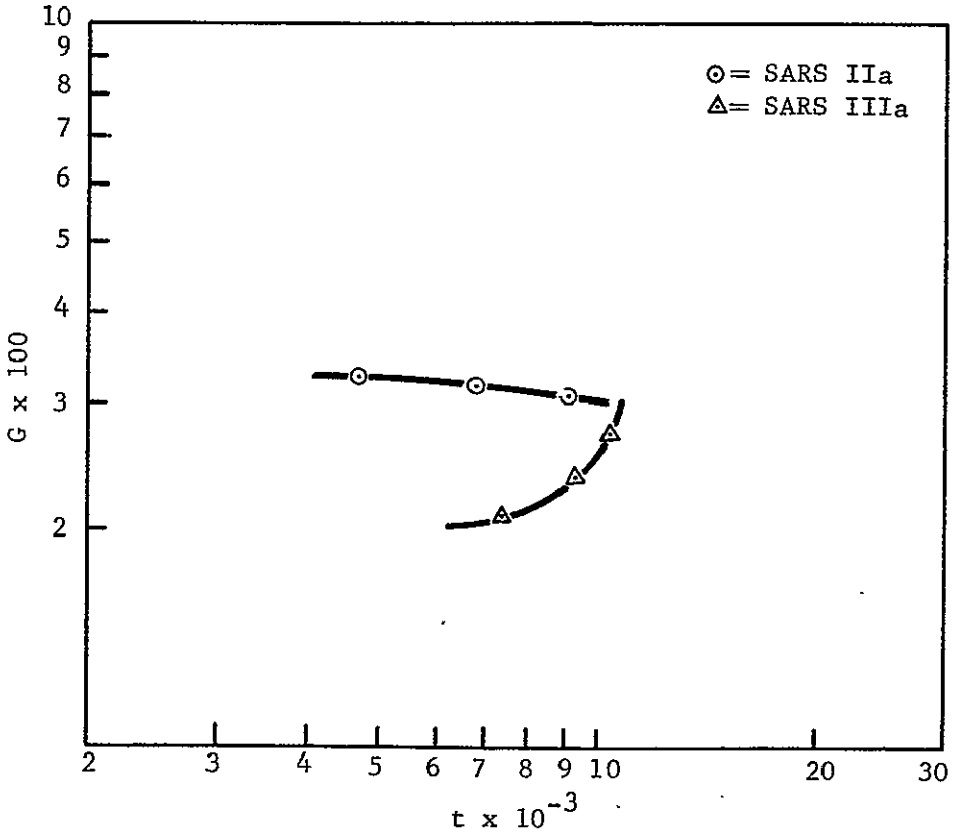

FIGURE 14 LD50 G versus Duration Curves for $+G_x$ Impact Orientation.

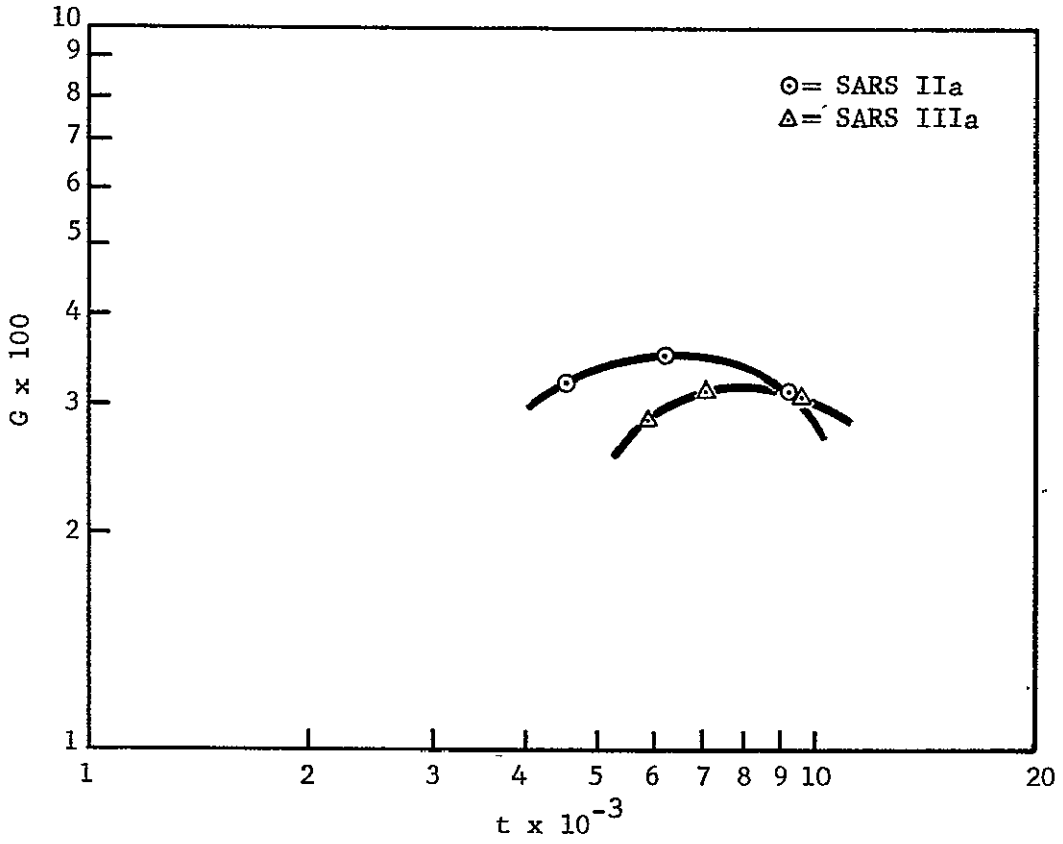

FIGURE 15 LD50 G versus Duration Curves for $-G_x$ Impact Orientation.

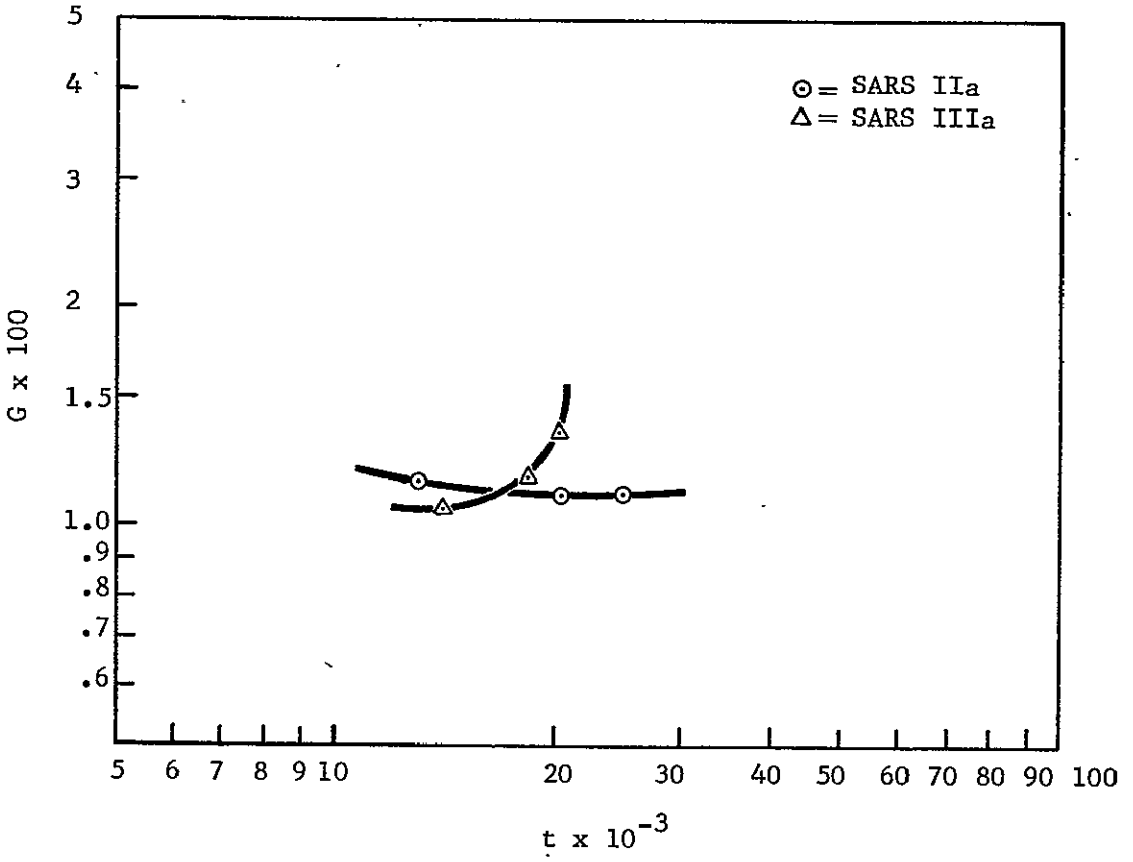

FIGURE 16 LD50 G versus Duration Curves for $+G_z$ Impact Orientation.

TABLE V INCIDENCE OF MAJOR PATHOLOGY IN NONSURVIVORS EXPOSED TO $+G_X$ IMPACT

	SARS IIIa			SARS IIa		
ENTRANCE VELOCITY (ft/sec)	40	60	80	40	60	80
TOTAL NONSURVIVORS	16	28	18	15	26	26
PATHOLOGY						
Pulmonary hemorrhage	16	20	15	15	26	26
Cardiovascular						
vena cava laceration at diaphragm	2					
vena cava laceration at caval/renal junction		17	3			
blood in pericardium			1			
Hepatic						
laceration	4	16	15			2
Gastrointestinal						
stomach hemorrhage		1	3	5	1	2
caecum hemorrhage	1			1	2	4
intestinal hemorrhage		4		2	1	2
stomach laceration			1			
Paralysis						
Brain						
hemorrhage	13	21	4	12	24	25
Other						
genital hemorrhage			2	1	2	1
subdermal hemorrhage thoracic region			1			
subdermal hemorrhage occipital region						1
spleen laceration		1				
renal vessel laceration	1	1				
rib fracture		3	3			

TABLE VI INCIDENCE OF MAJOR PATHOLOGY IN NONSURVIVORS EXPOSED TO-G_X IMPACT

	SARS IIIa			SARS IIa		
ENTRANCE VELOCITY (ft/sec)	40	60	80	40	60	80
TOTAL NONSURVIVORS	21	28	29	18	10	25
PATHOLOGY						
Pulmonary						
hemorrhage	21	24	26	16	8	15
laceration			1			
Cardiovascular						
vena cava laceration at entry to atrium				2	2	1
vena cava laceration at diaphragm	4	6	3			1
vena cava laceration at caval/renal junction		4	4		1	
pulmonary vein laceration		1				
aortic laceration						1
atrium laceration			2			2
ventricle laceration			1			
pericardium laceration			1			1
cardiac hemorrhage		1				
blood in pericardium					2	6
Hepatic						
laceration	19	23	23	7	3	14
Gastrointestinal						
stomach hemorrhage	3	2	6		1	2
caecum hemorrhage	4	15	7	1	1	4
intestinal hemorrhage	1	4	2			1
stomach laceration		1	3			
caecum laceration		2	7			
intestine laceration			1			
Paralysis						
Brain						
hemorrhage	11	9	12	9	4	9
Other						
jugular hemorrhage	5	8	8	14	7	17
axillary hemorrhage	4	10	16	14	6	21
subdermal hemorrhage thoracic region				1		1
diaphragm hemorrhage			1			
kidney hemorrhage	1		4			
hemorrhage around heart						4
muscle hemorrhage along spinal column					2	
genital hemorrhage	1		3	2		3
gall bladder hemorrhage						1
iliac hemorrhage	1	2	3			
urinary bladder hemorrhage			2			
spleen laceration	2	1	8		1	5
shoulder laceration			1			
forearm laceration		3	5			4
genital laceration				2		3
abdominal laceration without evisceration			1			
evisceration	1	2	6			
axillary laceration		1	1			
hindlimb fracture		1				1
forearm fracture			4			6

TABLE VII INCIDENCE OF MAJOR PATHOLOGY IN NONSURVIVORS EXPOSED TO $+G_Z$ IMPACT

	SARS IIIa			SARS IIa		
ENTRANCE VELOCITY (ft/sec)	40	60	80	40	60	80
TOTAL NONSURVIVORS	15	14	11	13	17	11
PATHOLOGY						
Pulmonary hemorrhage	13	10	9	3	6	4
Cardiovascular						
vena cava laceration at entry to atrium	2	3	2			
vena cava laceration at caval/renal junction		1				
azygos laceration		1				
aorta laceration		2				
atrium laceration	2	2	1			
cardiac hemorrhage	1	3				
pericardial laceration	2					
Hepatic						
laceration	1		1	1		
Gastrointestinal						
caecum hemorrhage	2		4			5
intestinal hemorrhage						2
Paralysis						
spinal fracture	1	1	4	3	5	8
undetermined	1	1	5	9	16	11
Brain						
hemorrhage	7	2	3	4	4	1
Other						
jugular hemorrhage	1	2		4	2	1
axillary hemorrhage	2			1	3	4
subdermal hemorrhage			1			1
subdermal hemorrhage thoracic region				1		4
retroperithoracic hemorrhage			1			
pelvic hemorrhage			2			
muscle hemorrhage along spinal column				1	1	2
rib fracture					3	1
hemorrhage around heart						2
genital hemorrhage						5

TABLE VIII TIME OF DEATH OF NONSURVIVORS

Death Occurred Within:	$-G_x$ Entrance Velocity and Type of SARS					
	40 ft/sec		60 ft/sec		80 ft/sec	
	IIIa	IIa	IIIa	IIa	IIIa	IIa
5 minutes	15	16	20	5	21	23
10 minutes	4	1	1			
30 minutes	1		3			
1 hour				2		
6 to 24 hours	1		4	2	1	2
Total	19	17	28	9	22	25
	$+G_x$					
5 minutes	16	14	23	25	11	26
10 minutes			1			
30 minutes			3	1	4	
1 hour						
6 to 24 hours		1	1		3	
Total	16	15	28	26	18	26
	$+G_z$					
5 minutes	15	13	14	17	11	11

(All $+G_z$ nonsurvivors either expired within 5 minutes or exhibited bilateral hindlimb paralysis immediately postimpact.)

Velocity change (ΔV) was calculated from

$$\Delta V = G_{avg} g(T_1 + T_2 + T_3) \tag{5}$$

Entrance velocity data were calculated from the sled transit time T_t over the last 3 inches before impact with the honeycomb column. The time values were taken from either a digital counter readout or from the oscillograph record where the same data were recorded graphically. Entrance velocity was determined by

$$V_e = \frac{1000}{4T_t} \tag{6}$$

where

V_e = entrance velocity in ft/sec

T_t = transit time over 3 inches in milliseconds

Each test condition included a statistical group of 40 animals; 20 at one G level and 20 at a second G level with the orientation, SARS, and entrance velocity held constant for all 40. The two data subgroups were each reduced to obtain a set of values for percent mortality, G_{avg}, G_{mp}, V_e, ΔV, impact duration, and onset. All values are averages for 20 exposures in each subgroup. Certain of these data for the two subgroups were then subjected to the probit transformation (Finney, 1962) as a means of approximating the impact dose level for 50% mortality. The probit transformation relates the percent mortality, in probit units, to the impact dose or G so that the typical sigmoidal response curve is expressed in terms of a linear equation of the general form

$$Y = 5 + \frac{1}{\sigma}(x - \mu) \tag{7}$$

where

Y = percent mortality in probit units

σ = variance of the distribution

μ = center of the distribution

x = dose (G)

The median lethal dose or LD50 is that value of x which gives Y = 5. A linear regression equation derived from the above expression is

$$Y = a + b \log x \tag{8}$$

where

a = constant for the intercept

b = slope constant for the regression line

Although the data from this investigation provided only two points for determination of a particular LD50 value, it was thought that the probit transformation would still be of value in correction of graphical plotting error due to the sigmoidal response characteristic, especially when one of the two data points lay at an extreme from the median. (The effect of the probit technique is naturally maximized with a greater number of data points.) The percent mortality and G_{avg} data for each of the 18 test groups were used to develop discrete regression equations for each group. Corresponding LD50 G levels were then obtained from the regression equations.

SECTION VI

DISCUSSION

The mechanisms of injury to a biological system exposed to impact are related to the impact energy functions, the support and restraint system variables (if any), and the orientation of the subject to the forcing function. By keeping all variables constant except one, the effect of this one variable upon the injury mechanisms can be studied. By alternating the variables to be studied, the most protective or least injurious exposure conditions can be determined. In this study, two types of support and restraint systems were compared in the $\pm G_X$ and the $+G_Z$ orientations, and impact entrance velocities of 40, 60, and 80 ft/sec using LD50 as the criterion. Thus, the basic variations were the support-restraint systems with the evaluation being conducted under the given test conditions. Although the test subjects were guinea pigs, the mechanisms of injury are, in the main, functionally relatable with those of man and the comparison of the two support and restraint systems should provide an insight into analogous human functional response.

PATHOLOGY

Gross pathological findings suggest that SARS IIa provided a greater degree of impact protection than did SARS IIIa. This was especially true with cardiovascular pathology and injury to abdominal viscera. Lung hemorrhage was the most frequently occurring injury under most of the impact conditions, regardless of the system used. The exception was in $+G_Z$ with SARS IIa where only 32% of the nonsurvivors exhibited this type of trauma. Brain hemorrhage occurred throughout the test program with the highest incidence found in $+G_X$. However, in most instances where brain hemorrhage occurred, other lethal injuries were found throughout the body. Hepatic laceration occurred most frequently with SARS IIIa, especially in $\pm G_X$. Incidence of cardiovascular pathology was higher with SARS IIIa than with SARS IIa. The highest incidence of injury to organs of the gastrointestinal tract occurred in $-G_X$ with SARS IIIa. Pathology of this type generally involved the caecum. Bilateral hindlimb paralysis was restricted to the $+G_Z$ orientation (spinal fractures were subsequently observed at autopsy). In the $+G_Z$ impact protection from lung hemorrhage and CVS injury in SARS IIa over that in SARS IIIa appears to have been made at the expense of the vertebral column. Tables IX and X give the percent occurrence of major pathology for 341 nonsurvivors in terms of separate and combined entrance velocities, respectively.

Pulmonary Hemorrhage

Lung pathology included petechial hemorrhage and acute surface hemorrhage involving entire lobes. Hemorrhage of varying degree was

TABLE IX PERCENT OCCURRENCE OF MAJOR PATHOLOGY IN NONSURVIVORS AT THREE ENTRANCE VELOCITIES

	IIIa			$-G_x$	IIa	
	40	60	80	40	60	80
Brain Hemorrhage	52	32	45	50	40	36
Pulmonary Hemorrhage	100	86	90	89	80	60
Cardiovascular Pathology	19	43	34	11	30	20
Hepatic Laceration	91	82	79	39	30	56
Gastrointestinal Pathology	43	89	90	6	20	28
Paralysis	0	0	0	0	0	0
	IIIa			$+G_x$	IIa	
Brain Hemorrhage	81	75	22	80	92	96
Pulmonary Hemorrhage	100	71	83	100	100	100
Cardiovascular Pathology	12	96	17	0	0	0
Hepatic Laceration	25	57	83	0	0	8
Gastrointestinal Pathology	6	18	33	53	15	31
Paralysis	0	0	0	0	0	0
	IIIa			$+G_z$	IIa	
Brain Hemorrhage	47	14	27	31	24	9
Pulmonary Hemorrhage	87	71	82	23	35	36
Cardiovascular Pathology	33	78	27	0	0	0
Hepatic Laceration	7	0	9	8	0	0
Gastrointestinal Pathology	13	0	36	0	0	64
Paralysis	7	7	45	69	94	100

TABLE X PERCENT OCCURENCE OF MAJOR PATHOLOGY - CUMULATIVE VELOCITIES*

	IIIa			IIa		
	$-G_x$	$+G_x$	$+G_z$	$-G_x$	$+G_x$	$+G_z$
Brain Hemorrhage	42	61	30	42	91	22
Pulmonary Hemorrhage	91	82	80	74	100	32
Cardiovascular Pathology	33	52	48	19	0	0
Hepatic Laceration	83	56	5	45	3	2
Gastrointestinal Pathology	77	19	15	19	30	17
Paralysis	0	0	18	0	0	80
Total Nonsurvivors		180			161	

*40 to 80 ft/sec entrance velocities.

more common in the periphery of the lobes and was occasionally seen in the hilum. No microscopic examinations were conducted during this program; however, this type of pathology has been previously studied in this laboratory and reported by Lombard (1964b). The latter investigation reported varying degrees of alveolar hemorrhage and areas of emphysyema adjacent to areas of atelectasis. In the $-G_x$ orientation the incidence of lung hemorrhage was high in both systems, occurring in 91% with SARS IIIa and 74% with SARS IIa. Many of the affected animals exhibited acute surface hemorrhage in areas adjacent to the ribs (rib marks). Injury to the periphery of the lobes was generally more severe than at the hilum. One case of lobe laceration occurred in a subject exposed in the 80 ft/sec regime. Lung hemorrhage occurred in all nonsurvivors in the $+G_x$ orientation with SARS IIa and in 82% with SARS IIIa. Hemorrhage was more frequent at the peripheral aspects of the lobes. The incidence of lung hemorrhage was greater in SARS IIIa than in SARS IIa in $+G_z$. Hemorrhage tended to be restricted to the lower aspects of the lobes adjacent to the diaphragm. In the $+G_z$ impact more protection was afforded the thoracic organs with the full torso restraint of SARS IIa than with the separate chest and pelvic strap restraint of SARS IIIa.

Cardiovascular Pathology

Cardiovascular pathology included trauma to the heart and the major blood vessels i.e., vena cava, aorta, and pulmonary vessels. Failure of the vena cava occurred with the greatest frequency. In lethal $-G_x$ exposures, the incidence of cardiovascular damage was relatively low for both systems, occurring in 33% with SARS IIIa and 19% with SARS IIa. SARS IIa appeared to provide a greater degree of protection to the vena cava than did SARS IIIa. Thirteen cases of laceration of the vena cava at the level of the diaphragm were noted with SARS IIIa, whereas this injury occurred only once with SARS IIa. This could be attributed to the support given the liver by the torso restraint of SARS IIa. The separate chest and pelvic restraints of SARS IIIa most likely allowed the liver a higher degree of relative movement during impact. The resultant displacement of this large organ with its considerable mass could apply shear forces on the vena cava in the area of hepatic attachment. These forces could account for the frequent incidence of laceration. The SARS IIa restraint minimizes liver displacement, thereby reducing shear forces on the vena cava. Eight cases of laceration of the vena cava occurred at its junction with the renal vein with SARS IIIa, whereas only one case was noted with SARS IIa. The SARS IIa restraint, by minimizing visceral displacement, may reduce the internal stresses responsible for injury to the major blood vessels in the abdomen. This increased protection afforded the abdominal blood vessels appeared to be at the expense of the thoracic vessels, suggesting a hydraulic compression wave. Five cases of laceration of the vena cava at the entrance to the atrium were noted with SARS IIa. This pathology was lacking with SARS IIIa. Laceration of the atrium was noted twice with each system. One case of pulmonary vein laceration and ventricular laceration occurred with SARS IIIa and one case of aortic laceration

occurred with SARS IIa. Hemorrhage was found in the area around the heart in four nonsurvivors with SARS IIa. The origin of this pathology was not found.

In $+G_x$ exposures, SARS IIa afforded a greater degree of protection to cardiovascular components than did SARS IIIa. No CVS damage occurred in nonsurvivors exposed in SARS IIa, whereas 52% of those tested with SARS IIIa showed evidence of trauma. The greatest incidence was in the 60 ft/sec runs where 10 cases of laceration of the vena cava occurred at the level of the diaphragm and 17 cases at the junction of the vena cava and the renal vein.

The full torso restraint provided by SARS IIa apparently prevented serious injury from occurring to the cardiovascular system in $+G_z$. No cardiovascular injury occurred in the 40 and 60 ft/sec experiments. In the 80 ft/sec tests, two nonsurvivors exhibited hemorrhage in tissues surrounding the heart but the site of injury was not determined. Of the nonsurvivors exposed to impact in the SARS IIIa, 48% exhibited CVS injury. This included seven cases of rupture of the vena cava at its entrance to the atrium, and one case of laceration at its junction with the renal vein. Five animals had atrial lacerations, and four cases of cardiac hemorrhage were recorded. Aortic lacerations occurred at the ascending portion of the vessel. Azygos laceration was reported once and two cases of pericardial lacerations occurred.

Hepatic Laceration

Varying degrees of laceration of the liver were observed. These ranged from small surface tears a few millimeters in length to subtotal hepatic mastication. In the $-G_x$ orientation hepatic laceration occurred more frequently with SARS IIIa (83%) than with SARS IIa (45%). The SARS IIIa restraint element evidently permitted a greater degree of liver displacement at impact,resulting in a higher incidence of hepatic mechanical trauma. High unit area force loading was evidenced by strap abrasions. With the SARS IIa restraint, liver displacement was apparently reduced by the more uniform restraint load distribution. Hepatic lacerations in the $+G_x$ orientation were observed in 56% of the nonsurvivors with SARS IIIa and only 3% for SARS IIa. Both of the cases occurring with SARS IIa were at 80 ft/sec. Liver damage occurred at all three velocities with SARS IIIa. With SARS IIIa, small lacerations occurred at the anterior margin of the liver near the exit of the vena cava in many subjects. The incidence of hepatic laceration was low for both SARS in the $+G_z$ orientation (5% for SARS IIIa and 2% for SARS IIa).

Gastrointestinal Pathology

Gastrointestinal pathology included hemorrhage and lacerations to organs of the GI tract, namely, the stomach, caecum, and intestines.

At $-G_x$ injury to gastrointestinal organs occurred in 77% of the nonsurvivors with SARS IIIa and in 19% with SARS IIa. The most commonly occurring pathology was hemorrhage of the caecum. Such hemorrhage was usually localized with no apparent preferential site. The caecum was generally well distended with fecal material in spite of the 24 hour fasting period before exposure. The position of the caecum relative to the SARS IIIa restraint was adjacent to the pelvic strap, which could possibly account for high area loading in this region. Laceration of the caecum occurred in nine animals exposed in SARS IIIa. Gastric laceration occurred with both SARS. Other pathology included hemorrhage of the intestines. Injury to organs of the gastrointestinal system were relatively few in number in the $+G_x$ orientation. Of the nonsurvivors, 19% sustained this type of pathology with SARS IIIa and 30% with SARS IIa. Four cases of gastric hemorrhage, and three cases of caecum hemorrhage were observed with SARS IIIa. One case each of intestinal hemorrhage and gastric laceration occurred. Eight cases of gastric hemorrhage and seven cases of caecum hemorrhage occurred with SARS IIa. Five cases of intestinal hemorrhage were also seen. Little injury occurred in the $+G_z$ orientation for either system. Gastrointestinal pathology for SARS IIIa was limited to six cases of caecum hemorrhage. Five cases of caecum hemorrhage and two cases of intestinal hemorrhage occurred in SARS IIa.

Paralysis

Animals surviving impact but exhibiting unremitting paralysis were categorized as nonsurvivors in accordance with the experiment procedure. Such animals were euthanized and autopsied in the usual manner. The category of paralysis does not include animals that, although expiring upon impact, may have suffered CNS damage that would have resulted in paralysis. Close examination of the spinal column was conducted on nonsurvivors to determine if vertebral failure had occurred. Spinal fractures were found in several, but not in all subjects where paralysis had occurred. Incidence of paralysis was markedly higher for SARS IIa (80%) than for SARS IIIa (18%). Most vertebral failures occurred in the thoracic segment of spinal column in both systems. One case of lumbar vertebral failure occurred with SARS IIa. Two animals that exhibited paralysis immediately postimpact recovered and were ambulatory by the end of the 24-hour survival period. Several animals exhibiting paralysis had no other apparent signs of injury.

Brain Hemorrhage

Early in the course of this work an improved mode of head support was developed in a separate laboratory effort to minimize frequency of nonsurvivors due to severe brain injury at relatively low G levels. With this improved head support, subsequent areas of hemorrhage were generally restricted to the surfaces of the cerebellum and the medulla oblongata. Brain hemorrhage as referred to herein refers to disruption of meningeal blood vessels, resulting in areas of hemorrhage on the surface of the brain.

In severe cases clots were present beneath the floor of the brain; on the surface of the cerebrum, medulla oblongata, and cerebellum; between the cerebrum and cerebellum; and in the longitudinal cerebral fissure.

In the $-G_x$ orientation, more animals exhibited brain hemorrhage with SARS IIIa than with SARS IIa; however, the percentage of nonsurvivors with this pathology was equal when the data from the different velocities were combined. Also, animals exposed in SARS IIa were subjected to higher G levels than those in SARS IIIa. In the $+G_x$ orientation, brain hemorrhage appeared in 61% of the nonsurvivors with SARS IIIa and 91% of the nonsurvivors with SARS IIa. Again, animals tested with SARS IIa were exposed to higher G levels than those impacted using SARS IIIa. The incidence of brain hemorrhage was relatively low for both systems in $+G_z$, occurring in 30% with SARS IIIa and 22% with SARS IIa.

Other Pathology.

In the $-G_x$ orientation, jugular and axillary hemorrhage were frequently observed in animals exposed in both SARS. These areas were adjacent to restraint straps, suggesting high surface tractions and induced shear stresses. Two animals with SARS IIIa had lacerations of the dermis in the axillary region. Three nonsurvivors tested with SARS IIIa sustained severe lacerations of the shoulder muscles. Splenic laceration occurred with both SARS. Renal hemorrhage occurred with SARS IIIa. Nine animals in SARS IIIa eviscerated at impact, resulting in severe trauma to abdominal viscera. Lacerations were located between the chest and pelvic straps in the region not supported by the restraint. No preferential direction of tearing was apparent, since lacerations extended longitudinally, laterally, and intermediately between these extremes. In many animals tested with SARS IIIa, fur adjacent to the straps was abraded. One subject had a longitudinal laceration of the dermis covering the abdomen but the muscle wall maintained its integrity. No eviscerations or indications of partial abdominal wall failure occurred with SARS IIa. Severe trauma to the forelimb was noted with both systems. Four subjects tested with SARS IIIa and six tested with SARS IIa sustained forelimb fractures. Dermal laceration of the forelimb occurred in eight animals with SARS IIIa and four with SARS IIa. These lacerations were located in the elbow region and ranged from simple tears to complete dermal severance around the limb with the dermis reflected back to the wrist. Survivors exhibited similar forelimb pathology. Three cases of forelimb fractures and one case of forelimb laceration were observed among the survivors with SARS IIIa. SARS IIa survivors sustained six cases of forelimb fractures. Among the nonsurvivors in $+G_x$ exposures six cases of rib fractures occurred with SARS IIIa. The spleen was injured in two cases and one case each of renal vessel failure and adrenal hemorrhage were seen with SARS IIIa. In $+G_z$ exposures, several animals that exhibited paralysis lacked any accompanying pathology. This occurred once with SARS IIIa and in ten cases with SARS IIa. Jugular and axillary hemorrhage occurred with both systems. Two animals impacted in SARS IIIa had severe hemorrhage

located retroperitoneally in the pelvic region. With SARS IIa two cases exhibited hemorrhage in the muscles along the spinal column but no evidence of fracture was found. Three cases of rib fracture were reported with SARS IIa.

Trends in Incidence of Pathology

The incidence or frequency of pathological categories for each of the 18 test combinations was studied to elucidate patterns correlatable with changes in entrance velocity, LD50 G level, duration, or other impact parameters with each particular SARS-orientation combination (see table IX). Pulmonary hemorrhage was the most uniformly appearing pathology across the spectrum of G levels and velocities. Except for a slight tendency towards increased occurrence at 40 ft/sec, the incidence of pulmonary injury in nonsurvivors remained fairly constant as velocity and G level were changed in each test combination. In the test combinations showing any incidnece of cardiovascular injury (all but SARS IIa, $+G_X$ and $+G_Z$), a marked peak in percent of occurrences was noted at 60 ft/sec. Although, in two of four of the combinations exhibiting this behavior, the LD50 G level was highest at 60 ft/sec. The trends in incidence of liver injuries varied greatly for each combination. In SARS IIIa at $-G_X$ the percent of occurrences was fairly constant for the span of G and velocities, while with SARS IIa in the same orientation the incidence rises with increasing velocity and correspondingly decreasing LD50 G. In $+G_X$ the frequency of hepatic injury rises directly for SARS IIIa with increasing entrance velocities and increasing LD50 G level, while for SARS IIa there was only negligble occurrence. Gastrointestinal injury generally increased in incidence with increasing velocity (but not LD50 G) in all test combinations. The exception was seen with SARS IIa in $+G_X$ where the highest incidence appeared at 40 ft/sec coinciding with the highest LD50 G level for this combination. Paralysis was restricted to subjects exposed to $+G_Z$ impacts and appears at a frequency directly proportional to LD50 G with SARS IIIa and inversely proportional to LD50 G with SARS IIa. In both cases, however, the variance is direct with velocity.

In sum, no strong or distinct patterns of incidence of pathology were readily correlatable to changes in G level or velocity or, in a more direct expression, to changes in the energy of the forcing function for a particular test combination. Over the range of impact variables studied, the trend in occurrence of pathology seems constant with few exceptions, especially if changes in occurrence of less than 10 to 20% are considered insignificant. Regardless of incidence trends, it is apparent that the survival limiting factors within the torso for SARS IIa are gross lung trauma in $\pm G_X$ (with hepatic injury influential in $-G_X$) and spinal damage in $+G_Z$. By comparison, the injury patterns seen with SARS IIIa in 50% mortality impacts are manifold in all three orientations.

STATISTICAL RESULTS

$+G_x$ Orientation

The results for impact exposures in the $+G_x$ orientation primarily reflect the action of the support element of each system. The comparative value of the two systems is, in fact, maximum in this orientation because of the high isovolumetric quality of the rigid, contoured SARS IIa support. The restraint elements play the lesser role of reducing lateral bulging or wraparound and rebound motion. The significant difference in LD50 levels between the two systems at all three velocity profiles points up the modification of failure mechanisms resulting from contoured support. The difference is greatest at the lower velocity, being about 117 G_{avg}. At 80 ft/sec the gap narrows to 40 G_{avg} suggesting a match point at some higher entrance velocity level. Comparison of the individual mortality curves for the two systems (see figures 8 and 9) shows the slopes for SARS IIa varying directly with velocity while the same data for SARS IIIa indicates no such dependence. Actually, only three of the nine sets of test conditions exhibit the expected linear dependence on velocity ($+G_x$ and $+G_z$ in SARS IIa and $-G_x$ in SARS IIIa). The G-t profiles for $+G_x$ further emphasize the approaching matchpoint and velocity independence of SARS IIIa. Two related mechanisms are suggested for the anomalous behavior of SARS IIIa in this orientation. First, the possibility exists that the somewhat narrow range of Δt's involved lay in or near a resonance boundary for SARS IIIa. Unfortunately, no data are presently available for resonance spectra of this particular SARS-animal system. If, however, a resonance mechanism is acting, the G-t data indicate its location near the shorter impact durations ($\approx$7 ms). The second related explanation involves the dependence of peak impact force in the system or either acceleration or velocity change. For a single-degree-of-freedom spring-mass system and rectangular pulse inputs, Stech and Payne*(unpublished) have shown that the peak force transferred to the system is a function of the velocity change when the pulse duration is shorter than the natural period of the system (t_n). Conversely, when the pulse duration exceeds the natural period, the peak force is directly related to peak pulse acceleration. Figures 17 and 18 illustrate the mortality regression curves for SARS IIa and IIIa strictly as a function of G. Figure 18 demonstrates the influence of G on mortality in SARS IIIa and strongly infers that t may be independent in this particular G-t representation. A third explanation may lie in the relatively narrow range of t explored and natural data scatter which could result. Kornhauser (1964), in his impact sensitivity work with mice, noted a similar discontinuity in the 50 to 80 ft/sec velocity change profile. With some reservations, he indicates the possibility of onset and pulse shape variations as causative mechanisms in his tests. The increased LD50 level of SARS IIa appears to be the product of a significant reduction in cardiovascular and hepatic injury in contrast to SARS IIIa. Concomitant with the abatement of trauma in these two areas, however, was a total occurrence of pulmonary injury at all three entrance velocities. The

*Ernest L. Stech and Peter R. Payne, Frost Engineering Development Corp., Contract AF 33(657)9514, unpublished data.

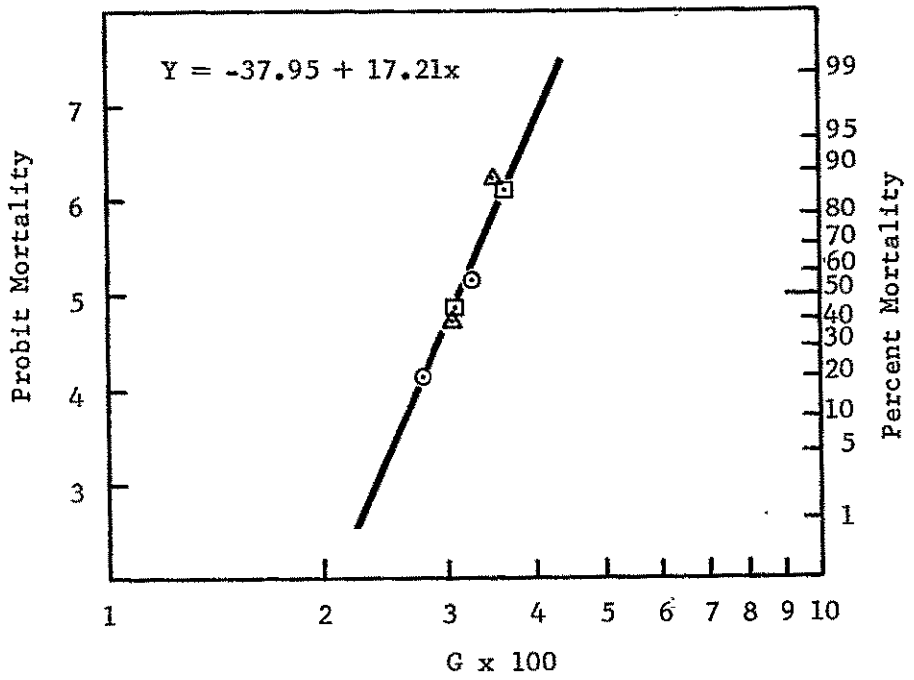

FIGURE 17 G versus Mortality, $+G_x$ Orientation, SARS IIa, Entrance Velocities of 40 to 80 ft/sec Inclusive.

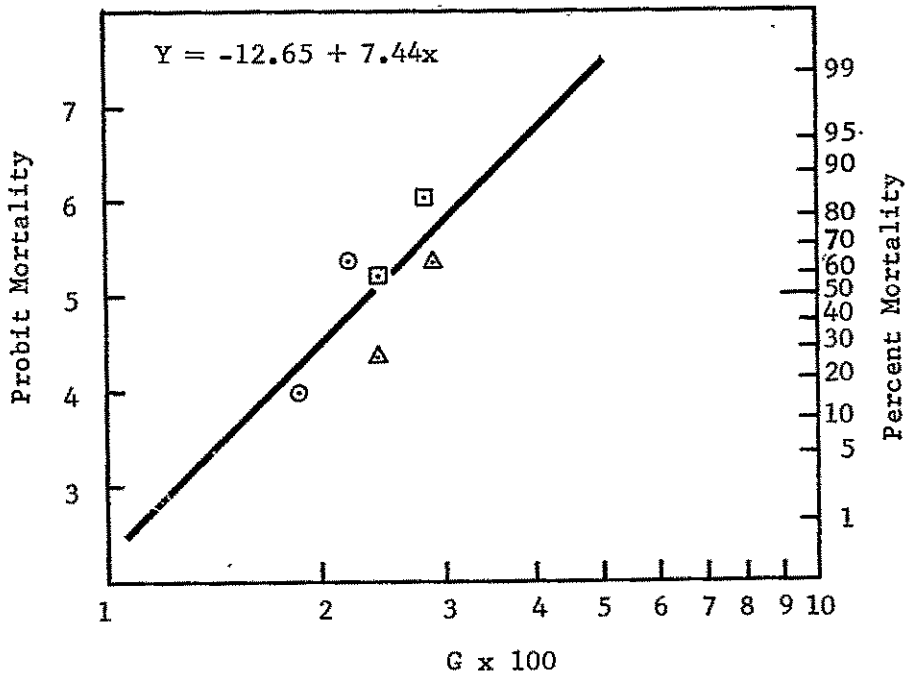

FIGURE 18 G versus Mortality, $+G_x$ Orientation, SARS IIIa. Entrance Velocities of 40 to 80 ft/sec Inclusive.

absence of lung laceration or rib fracture with SARS IIa suggests the mechanism of extreme thoracic pressure transients. The relatively high incidence of lung injury in SARS IIIa was accompanied by several cases of rib fracture due probably to the rapid plastic deformation of the torso against the flat support and the resulting surface tractions occurring in the descending chest strap regions.

$-G_x$ Orientation

Experiments in the $-G_x$ orientation provided data which, converse to $+G_x$, relate mainly to restraint element performance. Here, as expected, the performance gap is decreased to LD50 differentials of 38 G_{avg} at 40 ft/sec and 5 G_{avg} at 80 ft/sec. Examination of the SARS IIa and IIIa mortality curves (figures 10 and 11) shows a reversal in velocity dependence from that seen in the $+G_x$ data. Instead, SARS IIa indicates a discontinuity in the 60 ft/sec regime whereas SARS IIIa displays a direct velocity dependence. Again, this behavior may be traced to the relative velocity independence when $t>t_n$. The curves of mortality versus G_{avg} over the range of entrance velocities (figures 19 and 20) are practically equivalent in slope and intercept with SARS IIa having a 33 G_{avg} superiority in LD50 level for the summed velocities. The G-t profiles for $-G_x$ are exceptional in that they conform to the anticipated model response. Also, a matchpoint is seen at ≈ 9 msec duration. The pathology pattern for the two SARS are quite similar; the exceptions being gastrointestinal and, to a lesser extent, hepatic injuries. In general, the onset of mortal injury within the same pattern appears to be delayed in SARS IIa to a higher G level (modified slightly by the two exceptions). A notable aspect of the pathology trend seen in all three exposure orientations concerns the frequency of cardiovascular injury. In all cases where such pathology occurs, the highest incidence is seen in the 60 ft/sec entrance velocity range. (In two of these cases the maximum LD50 G level is also at 60 ft/sec.) With SARS IIa in $+G_x$ and $+G_z$ exposures, this pattern is absent because no cardiovascular injury was observed in these two test conditions. The primary failure mechanism in SARS IIa at this orientation appears to be centered in the cardiovascular system elements as witnessed by high incidences of jugular, axillary, coronary, and other great vessel injury. This response is in marked contrast to the general lack of cardiovascular trauma seen with SARS IIa in the $+G_x$ orientation where exposure G levels were comparable. The regular incidence of cardiovascular lacerations with SARS IIa in $-G_x$ points towards destructive tissue deformation in the hydraulic elements. The damping coefficient and natural frequency for the SARS IIa animal system would be lower in $-G_x$ impacts than in $+G_x$.

$+G_z$ Orientation

Experiments in the $+G_z$ orientation demonstrated the least disparity between the two systems. The mortality regression curves (figures 12 and 13) show a velocity dependence for SARS IIa and the opposite for SARS IIIa. At the lower velocity, SARS IIa is slightly superior while the LD50 values

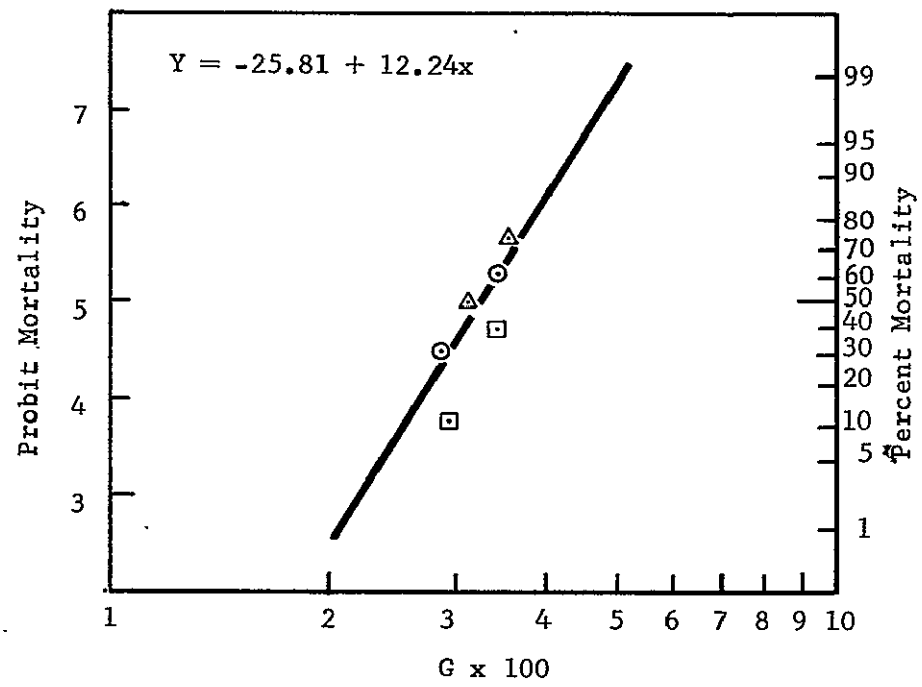

FIGURE 19 G versus Mortality, $-G_x$ Orientation, SARS IIa, Entrance Velocities of 40 to 80 ft/sec Inclusive.

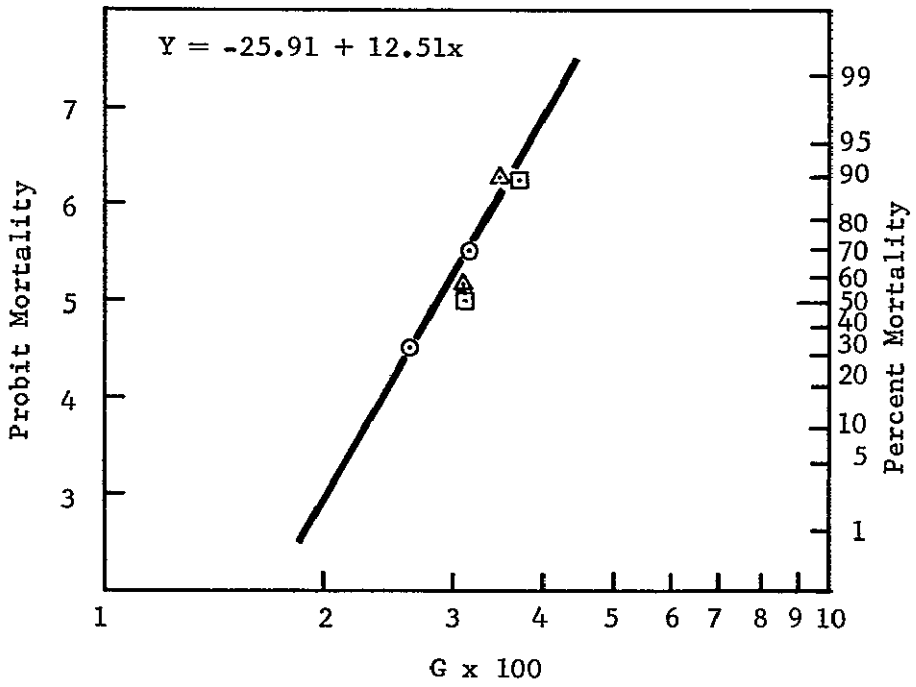

FIGURE 20 G versus Mortality, $-G_x$ Orientation, SARS IIIa, Entrance Velocities of 40 to 80 ft/sec Inclusive.

at 80 ft/sec entrance velocity indicate a marked improvement for SARS IIIa. In effect, the two systems almost balance out to equality over the velocity range. The G-t profiles for $+G_z$ (see figure 16) indicate a rapid performance shift for SARS IIIa at ≈20 msec. However, the degree to which mortality is a function of t for this condition is subject to question. The G versus mortality in $+G_z$ for cumulative velocities (figures 21 and 22) reveals an important point regarding SARS IIIa. The existence of data scatter and/or heterogenity is apparent, making a reliable performance estimate difficult. Coupled with this error factor is a striking difference in injury mechanisms between the two SARS. Thus, with the present data for $+G_z$, specific cross-correlation is of diminished value.

Initially we thought that the increased lateral support and restraint with SARS IIa would provide substantial "hoop tension", thus reinforcing the total torso-trunk column in compression loading. The increased Coulomb friction inherent in SARS IIa was also considered positive. These factors did not seriously alter the outcome in terms of an increased LD50 level; however, the injury mechanisms compared to SARS IIIa were significantly modified. The increased body column rigidity with SARS IIa evidently reflects directly on spinal column compression loading, producing a high incidence of paralysis. Neither system contained any padding or force attenuation media in the ishial tuberosity contact region. Both SARS "seat" or actually hind leg pans were composed of a flat 0.25 inch plywood spacer over the steel SARS frame.

The SARS IIIa permitted a greater degree of plastic deformation of abdominal and thoracic surfaces and contents. This is borne out directly in frequency of pulmonary, cardiovascular, and gastrointestinal injury. That the former two types of pathology predominated further indicates the possibility of an ascending compression wave trauma mechanism. Kazarian (1968) has reported on thoracic-abdominal compression waves due to $+G_z$ impacts in relation to vertebral body injury in small primates. The relatively low incidence of paralysis with SARS IIIa may indicate that certain injury modes are frequency sensitive since in the mechanically stiffer (and hence higher frequency) SARS IIa the injury pattern is reversed with a high paralysis rate and relatively low thoracic-abdominal injury.

ANALYTICAL CONSIDERATIONS

The basic components of the body such as bone, muscle, and ligament exhibit viscoelastic-plastic properties which can be defined by physical constants, such as bulk moduli, elastic moduli, shear moduli, yield values, and damping coefficients. It therefore appears logical that survival limits at different values of the forcing function variables, for similar injury mechanisms, can be studied by employing principles of mechanics.

In order to investigate the influence of support and restraint systems, orientation, and forcing function variables on survival, it is necessary

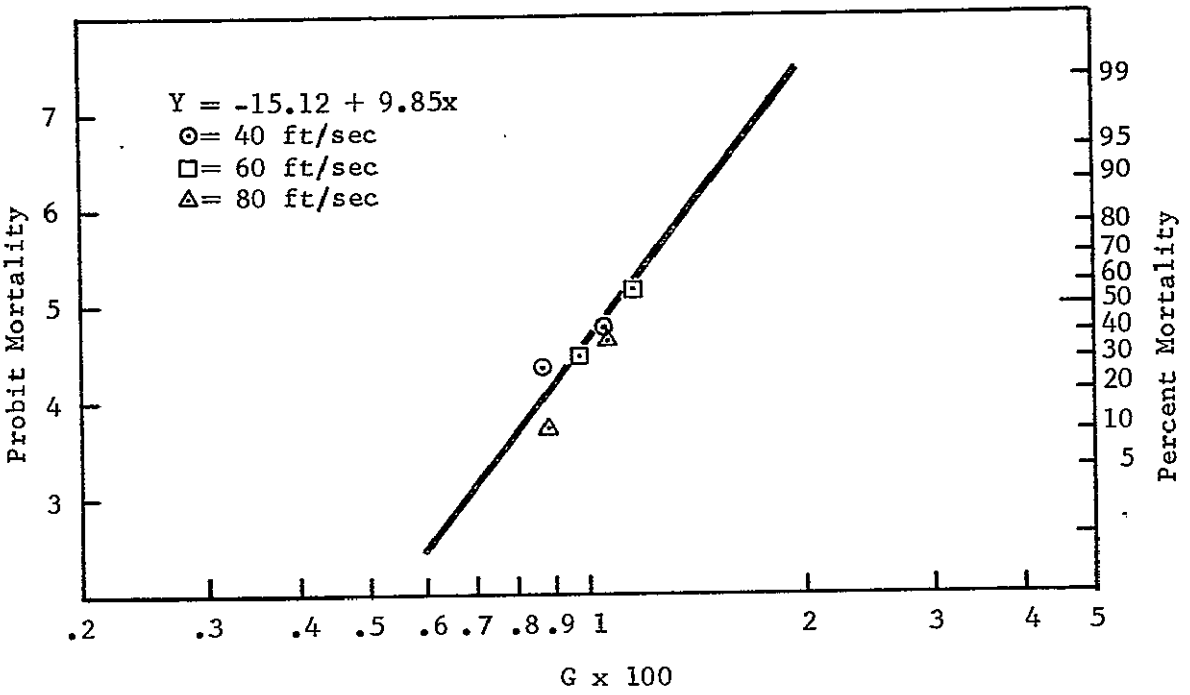

FIGURE 21 G versus Mortality, $+G_z$ Orientation, SARS IIa, Entrance Velocities of 40 to 80 ft/sec Inclusive.

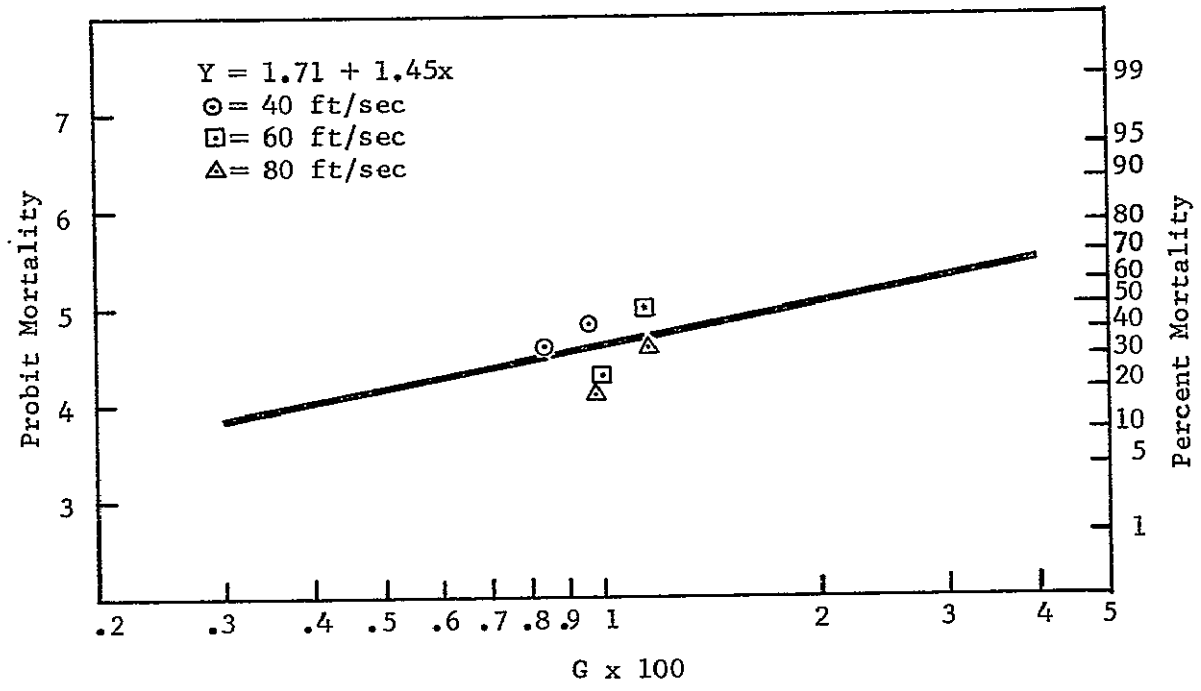

FIGURE 22 G versus Mortality, $+G_z$ Orientation, SARS IIIa, Entrance Velocities of 40 to 80 ft/sec Inclusive.

to consider the transfer of energy during impact. Energy transfer considerations are an essential prerequisite to a suitable formulation of a mathematical model of subjects exposed to impact acceleration.

Energy Transfer

To study the energy transfer during impact the energy change of sled or support and the transfer of energy between subject and restraint must be considered. The energy change of the sled or support is controlled by a forcing input to the sled as a known function of time. Energy profiles for a rectangular sled input are shown in figure 23 at velocity changes of 40, 60, and 80 ft/sec. A typical near rectangular pulse input is illustrated in figure 2A. In controlling the values of the forcing function variables for establishing LD50 curves, it is possible to vary G by keeping t constant, as shown in figure 24, or vary G by keeping ΔV constant, as shown in figure 25. The representative points on a G-t curve for these conditions are shown in figures 24D and 25D. Since the survival curves from previous laboratory data closely parallel the energy profile representation, use of the constant ΔV approach was highly desirable in economically limiting the number of animals used.

The rate of energy transfer between the subject and the restraint is governed by the properties of support and restraint, the value of the forcing function variables, and the orientation. The energy potential of mechanical forces producing impact injury is governed by two types of forces in dynamic equilibrium; transient body forces (inertia force-body volume) and transient surface tractions (force-surface area). Transient body forces from inertial loading perform work by inertial deformation. The potential W_{PB} of inertial loading is given by

$$W_{PB} = \int_V \vec{U} \cdot \vec{F} \, dV \tag{9}$$

where $\vec{U}$ is the displacement vector and $\vec{F}$ is the force vector over the volume V. The work of body forces produces organ laceration, tissue distortion, and vessel hemorrhage. Damage is assumed to be caused primarily by rotary inertia, hydraulic loading, bending and shear distortion effects.

Transient surface tractions from restraint loading perform work by compressing the base. The potential W_{PS} of surface loading is given by

$$W_{PS} = \int_S \vec{U}^n \cdot \vec{\tau}^n \, dS \tag{10}$$

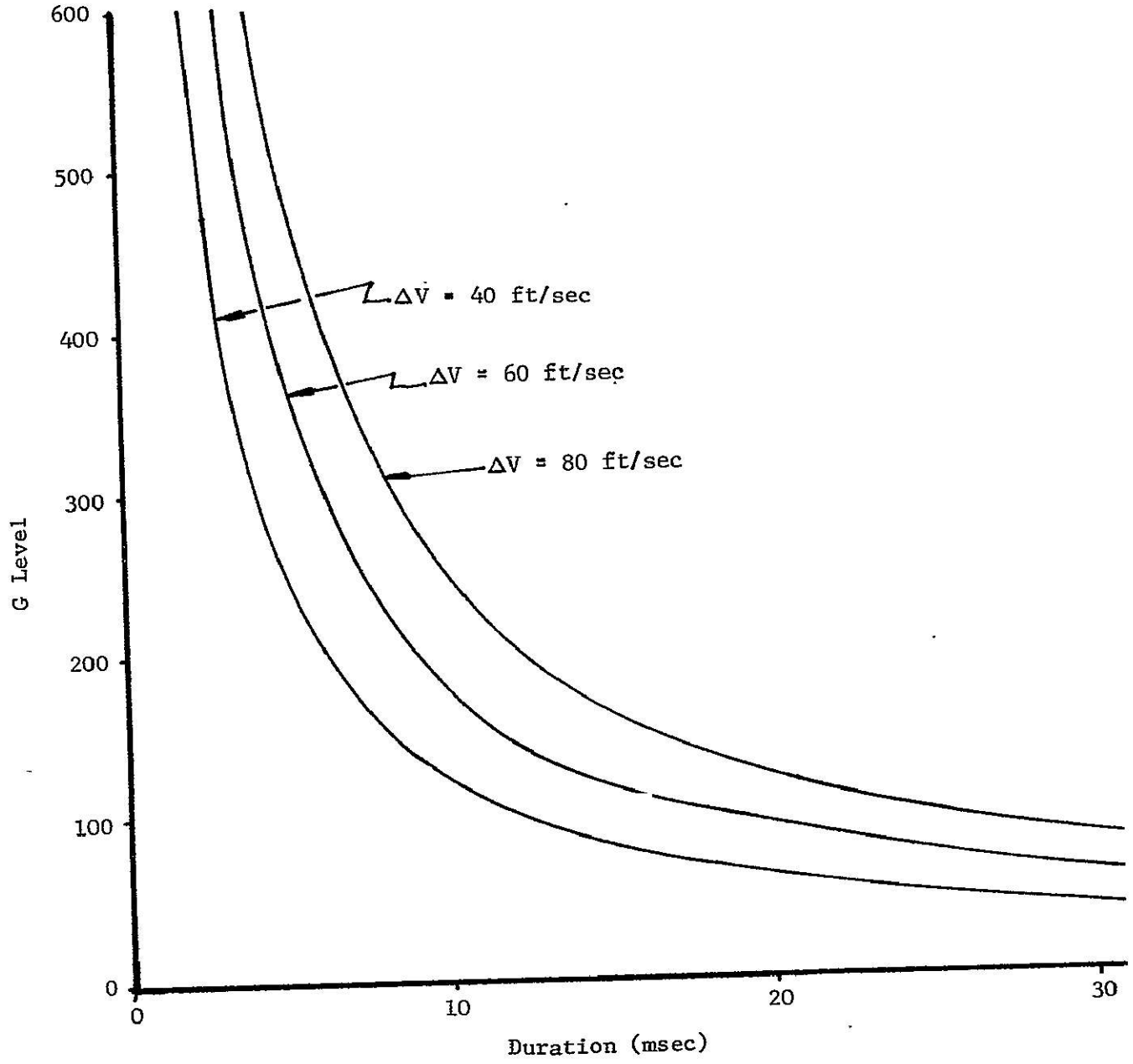

FIGURE 23 Energy Profiles

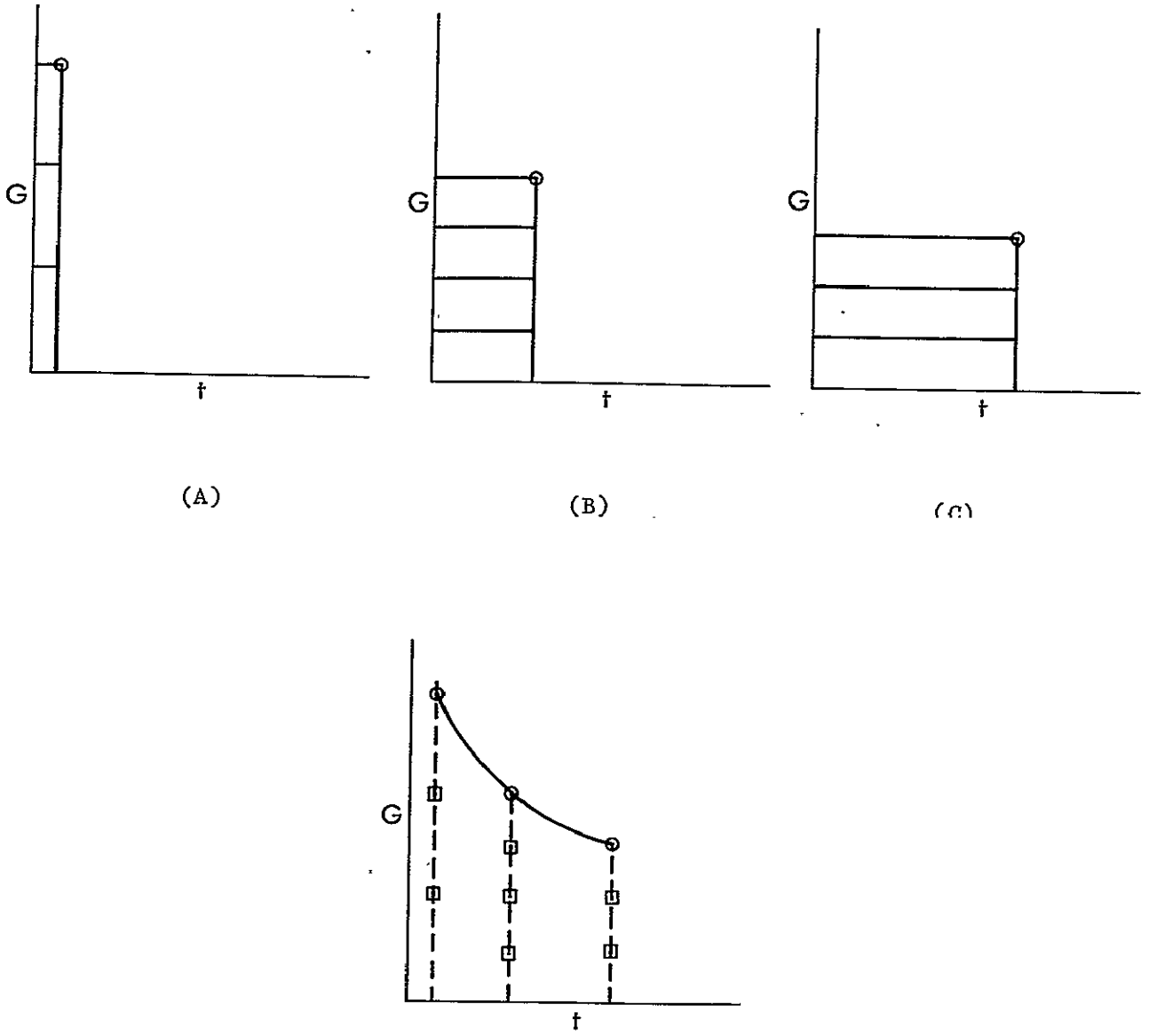

FIGURE 24 G-t Profile - Constant t

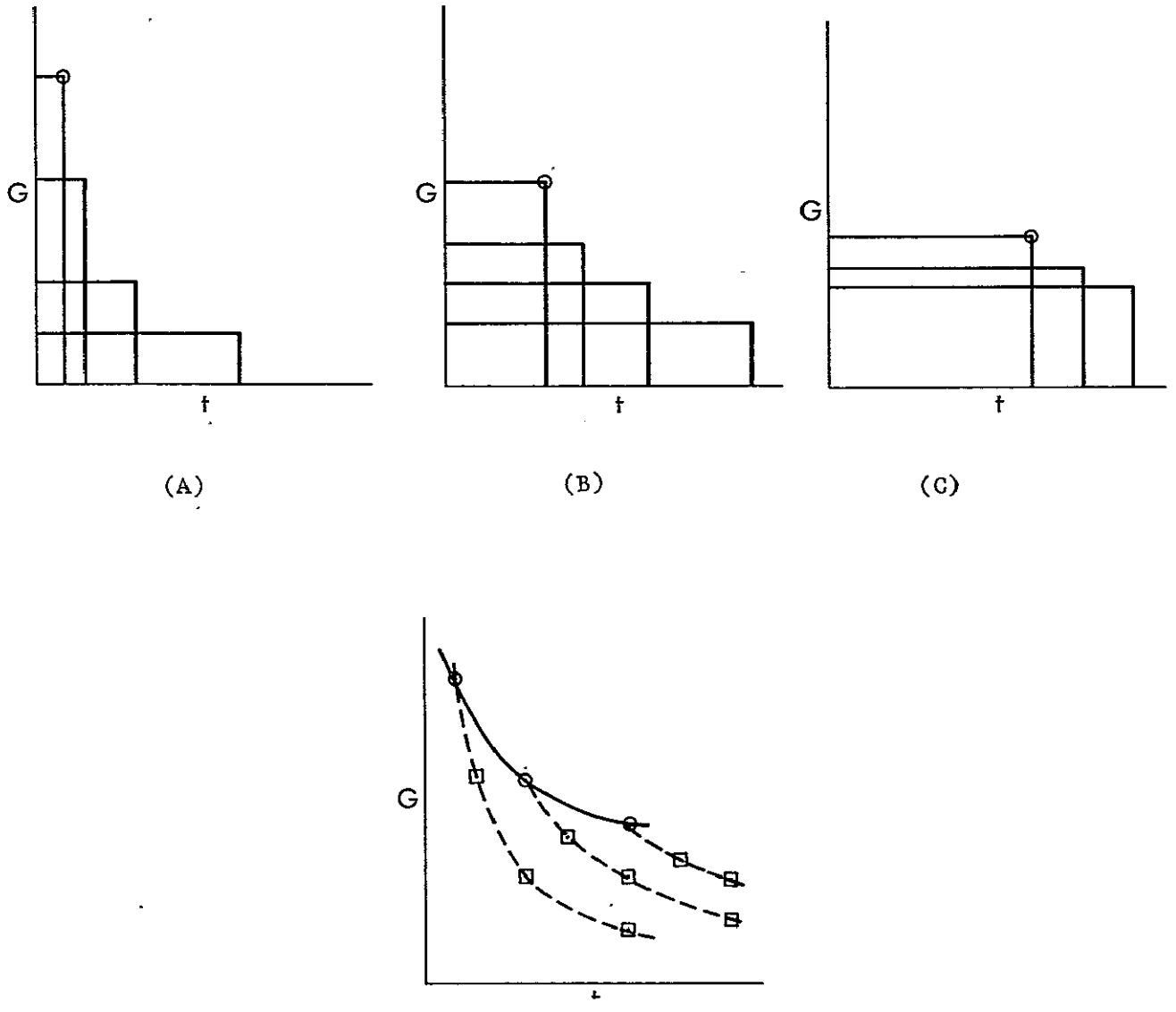

FIGURE 25 G-t Profile - Constant ΔV

where $\vec{U}^n$ is the surface displacement vector and $\vec{\tau}^n$ is the stress vector on the surface S. Surface tractions from restraint loading produce subdermal hemorrhage, contusions and organ laceration. Hydraulic and pneumatic pressure imbalances resulting from surface and/or body forces may account for a redistribution of blood volume within tissues with local areas of hemorrhage, ischemia, and fatal shock resulting.

Since the inertial forces and surface tractions are in dynamic equilibrium, a logical rationale for support-restraint design is to uniformly distribute the energy potential of mechanical forces by a uniform traction on the torso surface $\vec{\tau}^n$. This limits inertial deformations $\vec{U}$ well below the deforming destructive amplitude range and minimizes transient pressure imbalances.

Model Representation

Dynamic model concepts of subjects exposed to impact accelerations have been proposed by several investigators. Of particular interest is the damped spring mass system representation.

The well known investigations of Ruff (1950) indicate that tolerance limits of man for $+G_z$ accelerations, based on vertebral tolerance, have a plateau value of 20 G. The G-t profile illustrating these tolerance limits is shown in figure 26. Kornhauser (1964), using the spring mass analogy, has obtained a similar representation of the tolerance curves by his impact sensitivity method. This representation, characterized by two asymptotes, is based on the premise that below a certain G level no damage will occur, regardless of the duration or velocity change. It is evident from prolonged acceleration studies that his latter hypothesis fails. In addition, earlier work in this laboratory has disproven the other limiting assumption by experimentally demonstrating that damage is incurred in guinea pigs and monkeys for exceedingly small durations and large G.

Theoretical studies by Payne (1961) and other investigators (Stanley Aviation Company 1962) have demonstrated that a spring mass system approach can be used to correlate experimental data on human exposure. Experimental and analytical investigations by Lombard and Advani (1966) indicate that protective principles can be effectively studied by spring mass system representations. They indicate that isovolumetric containment of the torso can alter survival limits by 300% in some orientations at velocity changes of 40 ft/sec. The superior dynamic response of the isovolumetric system in their study is due to the increased frequency of lumped mass components and elastic elements. In the following discussion, the dynamic response of a damped spring mass system to a rectangular pulse is studied. Refinements of this system are also presented.

Consider the damped spring mass system shown in figure 27 subjected to a rectangular pulse of force P_o and duration t_1.

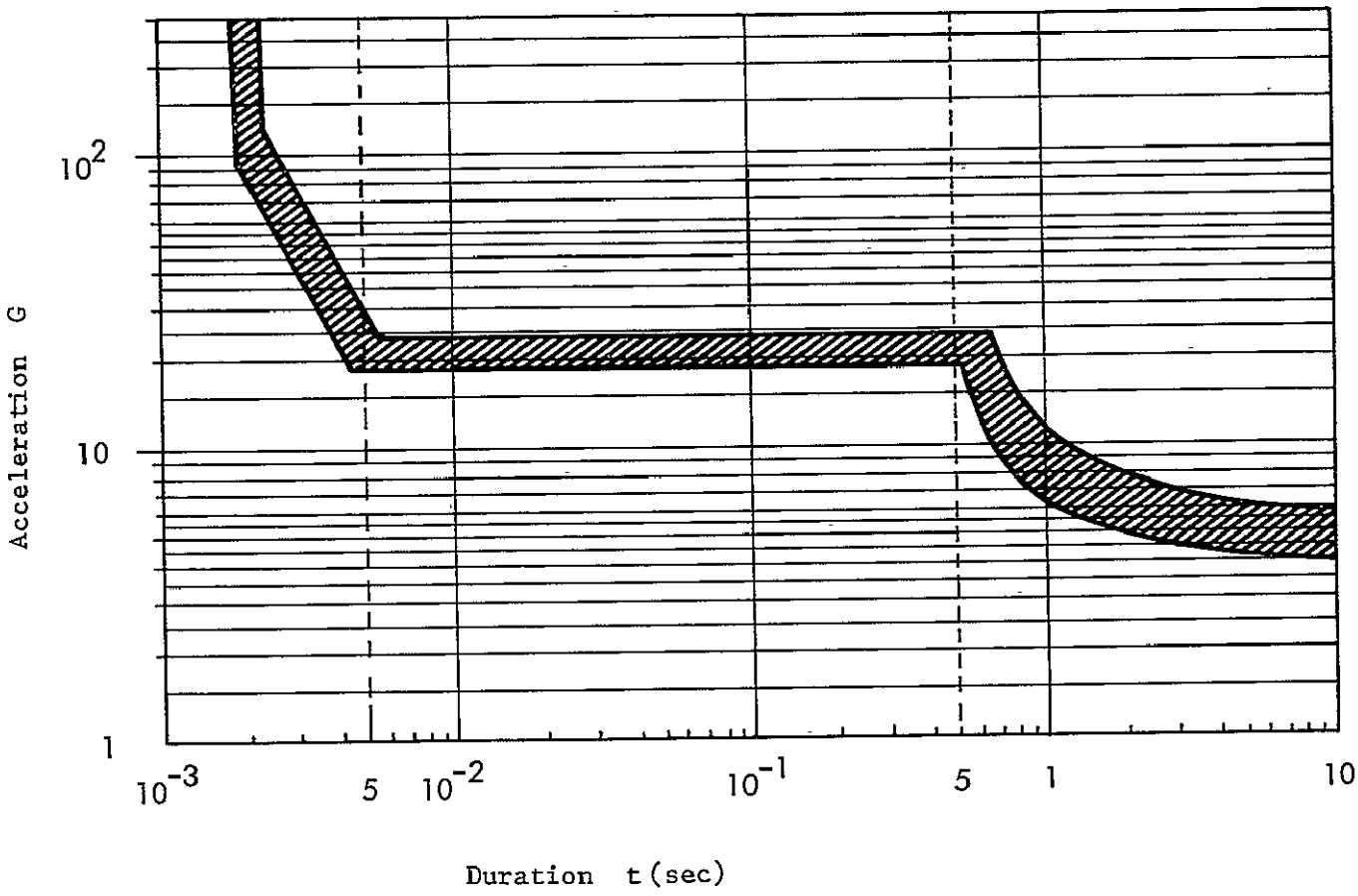

FIGURE 26 Tolerance Limits for $+G_z$ Accelerations

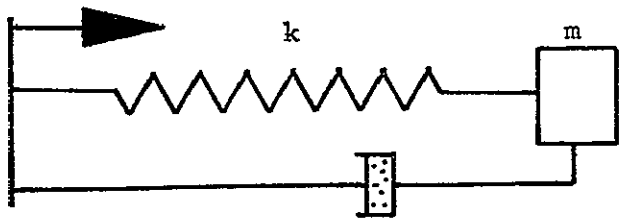

FIGURE 27 Damped Spring Mass System

The response of the system is given by

$$x = \frac{P_o}{k}\left[1 - \frac{e^{-\zeta\omega_N t}}{\sqrt{1-\zeta^2}}\cos\left(\sqrt{1-\zeta^2}\,\omega_N t - \Phi\right)\right] \quad 0<t<t_1$$

$$x = \frac{P_o}{k}\left(\left[1 - \frac{e^{-\zeta\omega_N t}}{\sqrt{1-\zeta^2}}\left(\cos\sqrt{1-\zeta^2}\,\omega_N t - \Phi\right)\right] - \left\{1 - \frac{e^{-\zeta\omega_N (t-t_1)}}{\sqrt{1-\zeta^2}}\left[\cos\sqrt{1-\zeta^2}\,\omega_N (t-t_1) - \Phi\right]\right\}\right) \quad t>t_1 \qquad (11)$$

where

$\omega_N = \sqrt{\frac{k}{m}}$ is the natural frequency of the undamped system

$\zeta = \frac{c}{2\sqrt{km}}$ is the damping factor

φ is the phase angle

The dynamic response factor for this system, for zero damping, is shown in figure 28.

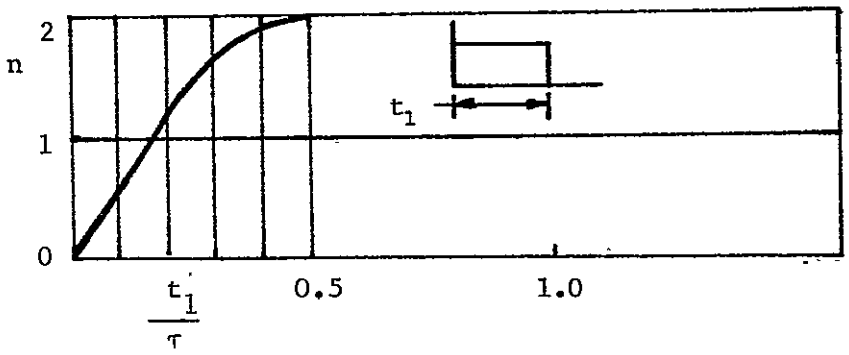

FIGURE 28 Dynamic Response Factor

A more realistic interpretation of the response is provided by replacing the linear, single degree of freedom system by

a. Multidegrees of freedom system
b. Continuous system (visco elastic rod)
c. Nonlinear system

The multidegrees-of-freedom system is a logical step in the refinement of the single-degree-of-freedom system, since it exhibits inertial coupling and elastic coupling characteristics. The general solutions for a pulse rectangular input of a two-degree-of-freedom system are reported by Lombard and Advani (1966). The natural frequencies in these studies have been taken from vibration and resonance studies of Goldman and Von Gierke (1961) and Coermann (1960).

Investigation by Hess (1956) indicates that the approximation of the human task by an elastic rod compares with ejection seat data. Attempts to approximate the human torso by viscoelastic rods have not yet been rigorously applied to man. Viscoelastic continuous systems appear to be potential candidates for mathematical model representations.

Since there is a considerable nonlinearity in the spring well below the deforming destructive amplitude range, a closer approximation is obtained by studying a nonlinear system with hardening characteristics. The equation governing motion of such a system is

$$\ddot{x} + \omega^2 (x + \beta x^3) + F(t) \qquad (12)$$

In general, no exact solutions exist for this equation. Approximate solutions for the transient response of this system to step excitations have been studied by Ergin (1956), Thompson (1960), Fung and Barton (1960).

GENERAL DISCUSSION

It is now evident from the data that the range of impact durations explored in the immediate work was not broad enough to provide accurate G-t representation in all systems and orientations. Further, it was not possible to develop discrete transfer functions for each system in each orientation and, concomitantly, the respective t_n's. Accordingly, it was deemed unwise to attempt development of a mathematical model without further additions to the data. In the G and ΔV regimes studied, however, the acceleration value appears to be the best single criterion of performance whereas ΔV and t assume a secondary level of significance. The criticality of velocity change on mortality seems to be seriously modified in the event of adequate support and restraint versus lack of any protective elements. Figure 29 compares data from Richmond (1961), on guinea pigs subjected to free fall impacts into a solid, flat surface, against data for SARS IIa and IIIa. The $-G_x$ orientation was assumed common and G was considered independent. Richmond's data are based on 57 exposures at impact velocities between 25 and 37 ft/sec while the combined SARS IIa and IIIa results reflect 120 exposures at entrance velocities between 40 and 80 ft/sec. Although Richmond gives no data regarding exposure G levels it is assumed that, in general, the animals exposed in the $-G_x$ orientation during the present work experienced a longer duration impact than would occur in free fall impact into a solid surface at the same entrance velocity.

Attempts were made during the course of the experimental effort to obtain data which would be useful in development of energy transfer functions between the decelerator sled and SARS-animal system. A miniature accelerometer was attached to the subject over the sternum, against the skin and insde the restraint webbing or apron. Typical results with this arrangement are shown in figure 30A for $+G_x$ and figure 30B for $-G_x$. These data indicate, to some extent, the amount of damping present in the SARS IIa-animal system for two different orientations. The smaller differential of 74 G_{mp} seen in $+G_x$ reflects the action of the animal and rigid support while the ΔG of 92 in $-G_x$ is indicative of the more resilient restraint. The natural frequencies of the same systems in the two orientations would differ correspondingly.

The data indicate that the general pattern and type of lethal injury mechanisms produced using the two systems differed in character to the extent that SARS IIIa exposures produced a higher incidence of specific trauma such as laceration, fracture, etc., while SARS IIa injury was less specific, i.e., general organ or regional hemorrhage. This suggests that the production of injury in SARS IIIa is largely a function of plastic deformation in direct point (surface tractions) loading with some degree of augmentation by indirect thoracic-abdominal plastic deformation resultir from compression wave propagation and the associated internal pressure gradients. The reverse appears true for SARS IIa injuries. This shift is evidently related to the decreased and relatively uniform load per

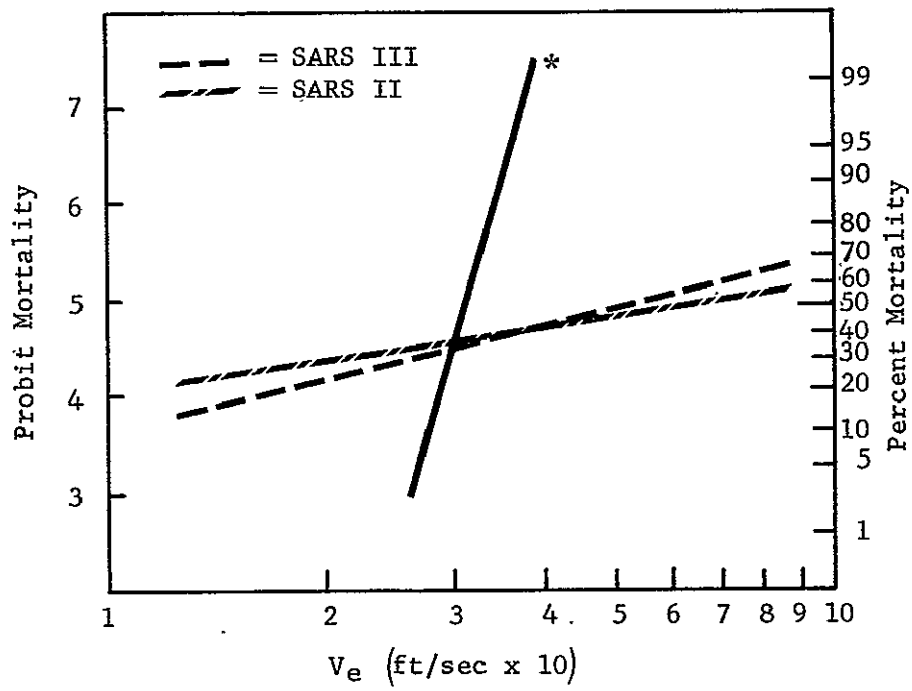

FIGURE 29 Probit Regression Lines for Entrance Velocity versus Mortality at 40, 60, and 80 ft/sec, $-G_x$ Impact Orientation.

* From Richmond (1961)

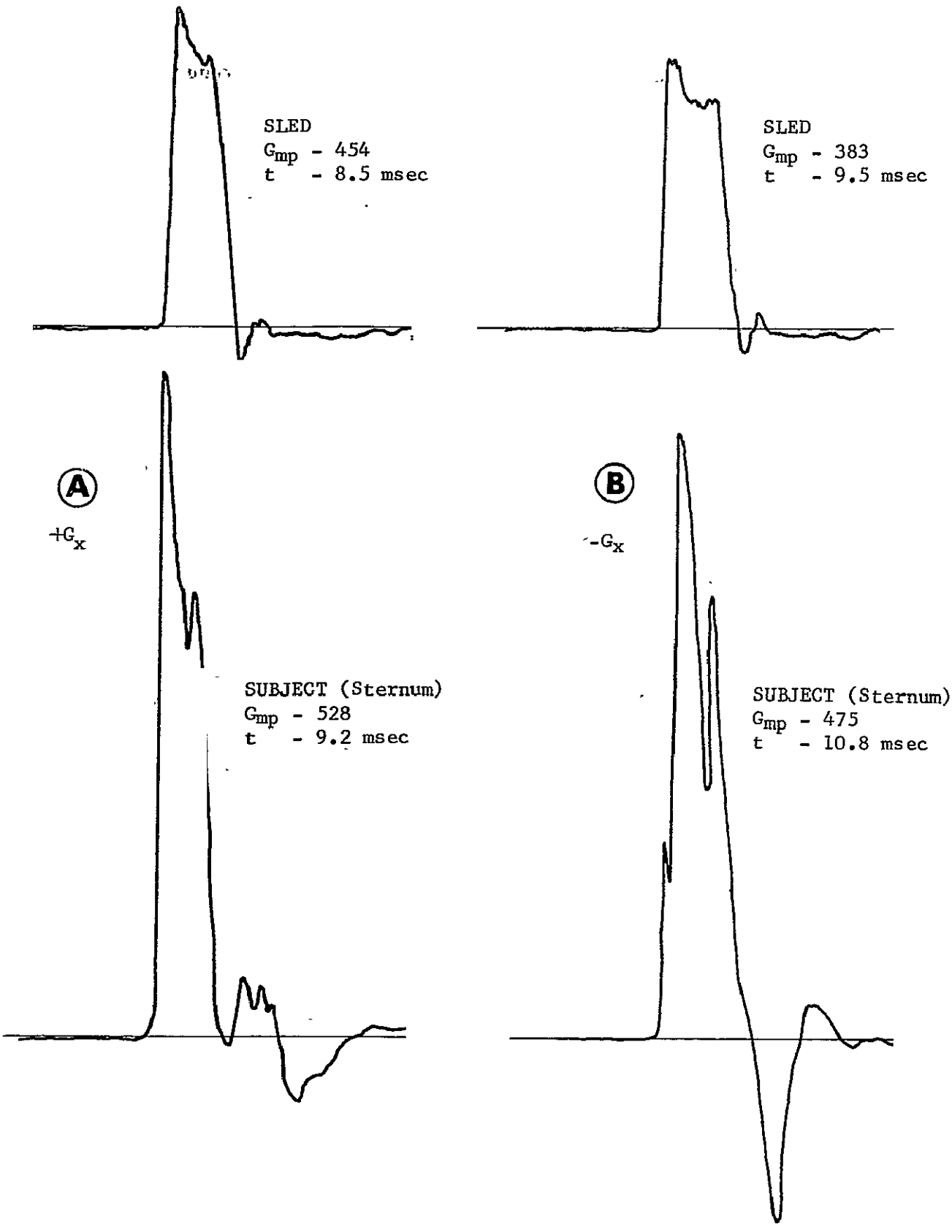

FIGURE 30 Comparison of Subject and Sled Acceleration - SARS IIa, $\pm G_x$, 80 ft/sec Entrance Velocity

unit area afforded by SARS IIa and to the increased frequency of the lumped mass components.

In general, results indicate a strong G dependence on mortality and a much less significant dependence on velocity over the range of G and ΔV studied. This may be partially reflected in the discontinuous LD50 response to input energy (expressed in terms of G-t) seen in SARS IIIa at $+G_X$ and $+G_Z$. The discontinuities may also be due to the inverse reason of critical t ($\approx t_n$) for those particular SARS-orientation conditions.

SECTION VII

CONCLUSIONS

Statistically significant data were obtained on the lethal impact dose for 50% of the guinea pig test subjects, using two types of support and restraint systems, three orientations, and three entrance velocities as fixed parameters.

a. The semi-isovolumetric SARS IIa concept provides superior impact protection in the $+G_x$ orientation over comparative conventional SARS concepts.

b. SARS IIa with its apron type restraint provides improved impact protection in the $-G_x$ orientation.

c. Although the SARS IIa greatly reduced cardiovascular injury in the $+G_z$ orientation a concomitant high incidence of spinal injury was incurred which, by definition, was considered nonsurvival. This factor militated against a comparative improvement in impact survival for SARS IIa.

d. Compared to previous guinea pig impact sensitivity data, both SARS IIa and IIIa showed respective increased LD50 G levels in $\pm G_x$ exposures as a result of maximized head protection.

SECTION VIII

RECOMMENDATIONS

Based upon the information acquired from this research effort the following overall recommendations are offered:

a. Additional research on the isovolumetric support and restraint-concept be conducted using larger animals and then man to establish survival and tolerance limits, respectively.

b. Support and restraint techniques for the head be improved for concomitant use with improved support and restraint systems for the torso.

c. Additional research on the isovolumetric support and restraint concept for $+G_z$ impact protection be conducted since it does minimize serious cardiovascular injury. Reduction of spinal injury may be possible with a force attenuator system.

REFERENCES

Coermann, R.R., G.H. Ziegenruecker, A.L. Wittwer, and H.E. von Gierke. The Passive Dynamic Mechanical Properties of the Human Thorax-Abdomen System and the Whole Body System. Aerospace Med., 31(6):443-455, 1960.

Ergin, E.I. Transient Response of a Nonlinear System by a Bilinear Approximation System. J. App. Mech., 23(4):635-641, 1956.

Fung, Y.C., and M.V. Barton. Shock Response of a Nonlinear System, J. App. Mech., 29(3):465-476, 1962.

Goldman, D.E., and H.E. von Gierke. Effects of Shock and Vibration on Man in Shock and Vibration Handbook, McGraw Hill Co., New York, 1961.

Hess, J.L. The Approximation of the Response of the Human Torso to Large Rapidly Applied Upward Accelerations by that of an Elastic Rod and Comparison with Ejection Seat Data, Report ES26472, Douglas Aircraft Company, El Segundo, California, 1956.

Kazarian, L.E., and H.E. von Gierke. Mechanics of Vertebral Body Injury in Monkeys as a Result of Spinal (+Z) Impact, AMRL-TR-68-83, Aerospace Medical Research Laboratories, Wright-Patterson Air Force Base, Ohio, 1968.

Kornhauser, M. Structural Effects of Impact, Spartan Books Inc., Baltimore, Md., 1964.

Lombard, C.F., P. Close, F.C. Thiede, and F.M. Larmie. Impact Tolerance of Guinea Pigs Related to Orientation and Containment, Aerospace Med., 35(1):1-6, 1964.

Lombard, C.F., S.D. Bronson, F.C. Thiede, P. Close, and F.M. Larmie. Pathology and Physiology of Guinea Pigs Under Selected Conditions of Impact and Support-Restraint, Aerospace Med., 35(9):860-866, 1964.

Lombard, C.F., A. Roy, J.M. Beattie, and S.H. Advani. The Influence of Orientation and Support-Restraint upon Survival from Impact and Acceleration, ARL-TR-66-20, Aeromedical Research Laboratory, Holloman Air Force Base, New Mexico, 1966.

Lombard, C.F., and S.H. Advani. Impact Protection by Isovolumetric Containment of the Torso, Proceedings Tenth Stapp Car Crash Conference, Holloman Air Force Base, New Mexico, 1966.

Payne, P.R. The Dynamics of Human Restraint Systems. Impact Acceleration Stress: Proceedings of a Symposium with a Comprehensive Chronological Bibliography, National Academy of Sciences National Research Council, Publication No. 977, pp 195-257, 1962.

Richmond, D.R., J.G. Bowen and C.S. White. Tertiary Blast Effects, Aerospace Med., 32(9):789-805, 1961.

Snyder, R.G. Human Tolerance to Extreme Impacts in Free-Fall, Aerospace Med., 34(8):695-709, 1963.

Shapland, D.J. A Study of the Dynamic Model Technique in the Analysis of Human Tolerance to Acceleration, Stanley Aviation Corporation Doc. No. 793, Denver, Colorado, 1962.

Stapp, J.P. Tolerance to Abrupt Deceleration, Collected Papers on Aviation Medicine, AGARDograph No. 6, Butterworth's Scientific Publications, London, pp 123-139, 1955.

Stapp, J.P. Analysis and Biodynamics of Selected Rocket-Sled Experiments, USAF School of Aerospace Medicine, Brooks Air Force Base, Texas, 1964.

Thomson, W.T. Shock Spectra of a Nonlinear System, J. App. Mech. 27(3):528-534, 1960.

Security Classification

DOCUMENT CONTROL DATA - R & D

(Security classification of title, body of abstract and indexing annotation must be entered when the overall report is classified)

1 ORIGINATING ACTIVITY *(Corporate author)* Northrop Corporate Laboratories 3401 W. Broadway Hawthorne, California	2a. REPORT SECURITY CLASSIFICATION Unclassified 2b. GROUP N/A

3. REPORT TITLE

DEVELOPMENT OF SUPPORT AND RESTRAINT TECHNOLOGY

4. DESCRIPTIVE NOTES *(Type of report and inclusive dates)*

Final Report, March 1967-July 1968

5. AUTHOR(S) *(First name, middle initial, last name)*

W.A. Robbins C.F. Lombard
G.L. Potter

6 REPORT DATE April 1969	7a. TOTAL NO. OF PAGES	7b. NO. OF REFS 20
8a. CONTRACT OR GRANT NO. F33615-67-C-1651 b. PROJECT NO. 7231 c. Task No. 723101 d.	9a. ORIGINATOR'S REPORT NUMBER(S) NCL 68-81R 9b. OTHER REPORT NO(S) *(Any other numbers that may be assigned this report)* AMRL-TR-68-136	

10. DISTRIBUTION STATEMENT

This document has been approved for public release and sale; its distribution is unlimited.

11. SUPPLEMENTARY NOTES	12. SPONSORING MILITARY ACTIVITY Aerospace Medical Research Laboratory, Aerospace Medical Div., Air Force Systems Command, Wright-Patterson AFB, OH 45433

13. ABSTRACT

Guinea pigs were exposed to backward and forward facing (±Gx) and tail first (+Gz) impact accelerations in two types of support and restraint systems at entrance velocities of 40, 60, and 80 ft/sec. After exploratory experiments to determine the approximate 50% lethal G level (LD50), estimates of G levels for 40 and 60% mortality were made and 20 guinea pigs were exposed at each level. This was accomplished for each orientation at each velocity in each of the two systems. Using probit analysis, the refined LD50 G level was calculated and the results tabulated for comparison of the two systems for survival potential. Regarding protection, the system employing the isovolumetric principle was markedly superior in +Gx impacts, slightly superior in -Gx impacts, and approximately equal in the +Gz orientation. Protection of the cardiovascular system by the isovolumetric system was markedly superior in +Gx and +Gz impacts but only slightly better in -Gx impacts. Comparison of the two thoracic-abdominal systems was made possible by the concomitant use of a previously developed support and restraint system for the head. The LD50 values using average G ranged from 209 to 325 for +Gx, 287 to 350 for -Gx, and 103 to 135 for the +Gz.

DD FORM 1 NOV 65 1473

Security Classification

14. KEY WORDS	LINK A		LINK B		LINK C	
	ROLE	WT	ROLE	WT	ROLE	WT
Impact accelerations Lethal Dose 50 Percent of Guinea Pigs Two Support and Restraint Systems Headward, Backward, Forward Accelerations						